Deltares

Modelling morphodynamics in the presence of immobile sediment

Model testing and sensitivity analysis

Modelling morphodynamics in the presence of immobile sediment

Model testing and sensitivity analysis

Authors
Victor Chavarrias
Willem Ottevanger

Modelling morphodynamics in the presence of immobile sediment

Model testing and sensitivity analysis

Client	Rijkswaterstaat
Contact	
Reference	
Keywords	

Document control	
Version	1.0
Date	2021-06-30
Project number	11206793-014
Document ID	11206793-014-ZWS-0002
Pages	63
Status	final

Author(s)		
	Victor Chavarrias	Deltares
	Willem Ottevanger	Deltares

Doc. version	Author	Reviewer	Approver	Publish
1.0	Victor Chavarrias	Kees Sloff	Johan Boon	

Executive summary

Rivers predominantly flow over the sediment that they transport. The transport of sediment causes changes in bed elevation with time. Moreover, sediment is seldom unisize and is usually comprised of a mixture of different sizes. The different mobility of fine and coarse sediment causes that the transport not only induces changes in bed elevation but also in grain size distribution. Worded differently, the bed surface becomes coarser or finer with time as the flow changes.

A relevant morphodynamic process occurring in alluvial rivers is the formation and break-up of coarse layers. Under low-flow conditions, the coarsest fractions are too large to be transported and remain immobile forming a coarse layer while the finest fractions are transported over them in bedforms such as dunes. Under high-flow conditions, coarse sediment is mobilized, suddenly entraining sediment that was protected below the coarse layer.

Rijkswaterstaat, as the authority managing the Dutch river system, is in charge of guaranteeing, among other things, safe, navigable, and ecologically-rich rivers. Accurately predicting the morphodynamic development of rivers is key in properly managing them. This comprises not only predicting the intrinsic behaviour, such as changes associated to flood events, but also the long-term effect of interventions for improving the river system, such as nourishments for limiting the existing degradational trend.

For a better management of the river system, Rijkswaterstaat is interested in improving the tools available for predicting morphodynamic changes. As such, an attention point is prediction of the formation and break-up of coarse layers. While there are modelling concepts available, these present several limitations. A new modelling concept was recently devised that is capable of better capturing the transport of fine sediment over a coarse layer as well as break-up and entrainment of coarse sediment under high-flow conditions. Nevertheless, this new modelling concept has not been widely applied. Prior to its general application it is necessary to gain knowledge and understanding of its features.

In this project, the new modelling concept is applied to a laboratory experiment to evaluate the capacity of the model against detailed measurements. Subsequently, the model is applied to idealized cases in which the effect of the model parameters is studied in detail. Finally, implications for field cases are derived.

Contents

1 Introduction

The two state-of-the-art models for predicting morphodynamic changes in the presence of immobile sediment (i.e., the Struiksma (1999) and the Hirano (1971) models) present several caveats. These limitations were studied by Chavarrías *et al.* (2020). In essence, the model by Struiksma (1999) captures morphodynamic development in the presence of an immobile sediment layer, but does not model break-up of the coarse layer. Moreover, the grain size of the material forming the coarse layer does not affect transport of sediment on top of it, which is not realistic.

The active-layer model captures formation and break-up of an armour layer implicitly only. The coarse layer is lumped into the active layer and immobile sediment remains part of the active layer. Hence, break-up and formation of a coarse layer can only be interpreted from the coarsest fractions of the sediment mixture becoming mobile or immobile.

Chavarrías *et al.* (2020) proposed an alternative modelling strategy, the HANNEKE model, specific for dealing with mixed-size sediment under conditions in which some of the sediment size fractions in a mixture are not mobilized by the flow. The main benefit of the HANNEKE model is that, contrary to the active-layer model is explicitly models the formation and break-up of a coarse layer underneath migrating bedforms.

The HANNEKE model has not been widely applied. For this reason, prior to application to field cases and projects, here understanding of the model is gained by means of application to a laboratory case and idealized cases.

2 Objective and research questions

The objective is to develop guidance for modelling based on:

- selection of modelling approach,
- key parameters to be considered,
- realistic ranges for these parameters,
- approach to calibration.

The following research questions arise:

1 Under which conditions is the HANNEKE model suitable and necessary?
2 What are the essential differences compared to the state-of-the-art model (i.e, the active-layer or Hirano model)?
3 Which are the most relevant parameters of the HANNEKE model and what is their role?
4 How sensitive are the results to variation in the model parameters?
5 How should the model parameters be chosen?

The ultimate goal is to provide recommendations for real field applications.

The report is organized as follows. In Section 3 the model is applied to a laboratory experiment on formation and break-up of an armour layer. In Section 4 the key model parameters are identified and varied in an idealized one-dimensional set-up that facilitates understanding. In Section 5 the model is applied to an idealized two-dimensional set-up for understanding the consequences of the modelling choices in the 2D pattern. Finally, in Section 6 the field implications are derived.

3 1D laboratory set-up

Klaassen *et al.* (1986) and Blom *et al.* (2003) conducted a similar set of laboratory experiments using mixed-size sediment. A step-wise hydrograph was imposed such that both initially and at the end stages only a part of the sediment mixture was mobile while the bed shear stress during a middle stage was sufficiently large to mobilize all sediment. During the initial low-flow conditions an armour layer formed which broke during the high-flow conditions and reformed at a lower position during the final low flow conditions (see Table 1).

Such experimental data-set is ideal for testing the different modelling concepts and their ability in reproducing measured data. The experimental data-set by Blom *et al.* (2003) may be more suitable than that by Klaassen *et al.* (1986) due to the more modern measurement equipment used by the former.

It is relevant to take into consideration that the conditions of the initial phase of the experiment by Blom *et al.* (2003) yield an ill-posed mathematical model (Chavarrías *et al.*, 2019). It may be necessary to slightly modify the grain size distribution or the load relation to obtain a well-posed model.

In this section the experiment of Blom *et al.* (2003) is rerun using the approach of Hirano (1971) and the modified Tuijnder approach of Chavarrías *et al.* (2020). The first phase (T5) of the experiment is used to calibrate the transport. The T5 experiment is run until equilibrium and the bed information is transferred to the simulation of the next phase T7. A photo of the equilibrium situation in T7 is shown in Figure 3.1. The T7 simulation has a higher discharge, and when it is completed the composition data is transferred to T9 (which is roughly the same discharge as T5).

Figure 3.1 Bed form pattern from T7 experiment at equilibrium conditions (from (Blom *et al.*, 2003))

3.1 Experimental setups

In Table 1 an overview is given of the experiments used for the 1D laboratory set-up.

Case	Discharge [m^3/s]	Depth [m]	Width [m]	Chézy [$m^{0.5}$/s]	Slope [‰]	q_b [10^{-5} m^2/s]	Dune height [m]
T5	0.254	0.245	1.5	37	1.5	3.15	0.038
T7	0.419	0.3362 (0.354)	1.5	37 (36)	1.5	5.46	0.066
T9	0.254 (0.272)	0.245 (0.260)	1.5	37 (34)	1.5	3.77	0.038

Table 1 Conditions of the T5, T7 and T9 experiments of Blom *et al.* (2003) as modelled in the current report. In brackets are the values reported in Blom *et al.* (2003).

The model is a one cell wide grid with a total length of 50 m and a width of 1.5 m. The number of grid cells along the length of the flume is 100. The initial sediment composition is prescribed as bed load sediment fractions where the finest diameter is 0.31 mm and the coarsest is 15.7 mm (Table 2). These are obtained from the measured data.

fraction	characteristic grain size d_k [m]
1	0.00031
2	0.00036
3	0.00040
4	0.00045
5	0.00053
6	0.00067
7	0.00010
8	0.00017
9	0.00294
10	0.00474
11	0.00667
12	0.00831
13	0.01050
14	0.01358
15	0.01576

Table 2 Characteristic grain sizes of the model of the experiments by Blom *et al.* (2003).

3.2 Calibration

The transport in the T5 simulations is calibrated for the transport formula of Meyer-Peter and Müller (1948) which reads:

$$Q_{\mathrm{b}k} = \begin{cases} \frac{\sqrt{g\Delta d_k^3}}{1-p} A_{\mathrm{cal}} \left(\theta_k - \xi_k \theta_{\mathrm{c}}\right)^B & \text{for } \theta_k - \xi_k \theta_{\mathrm{c}} > 0 \\ 0 & \theta_k - \xi_k \theta_{\mathrm{c}} \leq 0 \end{cases}, \tag{3.1}$$

where $Q_{\mathrm{b}k}$ is the sediment transport capacity including pores, g =9.81 m/s^2 is the acceleration due to gravity, $\Delta = (\rho_{\mathrm{s}} - \rho_{\mathrm{w}})/\rho_{\mathrm{w}} = 1.65$ is the relative sediment density, $\theta_k = u^2/\left(C^2 \Delta d_k\right)$ [-] is the non-dimensional bed shear stress of size fraction k, $\theta_{\mathrm{c}} = 0.047$ [-] is the critical non-dimensional bed shear stress, u [m/s] is the mean flow velocity, ξ_k [-] is the hiding-and-exposure coefficient, A [-] is the prefactor of the sediment transport relation, and $B = 1.5$ [-] is the power of the excess bed shear stress. The ripple factor, which multiplies the bed shear stress and account for the effect of bedforms on the formula, has been set to 1 for simplicity. The calibration then takes into account the effect of the ripple factor.

The sediment transport is complemented by a hiding-and-exposure correction function by Parker and Klingeman (1982):

$$\xi_k = \left(\frac{D_{\mathrm{m}}}{d_k}\right)^{A_{\mathrm{SKLHE}}}, \tag{3.2}$$

where D_{m} [m] is the mean grain size and b [-] is a parameter which determines the degree to which sediment is influenced by hiding and exposure. The geometric mean grain size may better represent the mean properties of the mixture but as this is not implemented in Delft3D, the arithmetic mean grain size is used.

Other hiding-exposure formulations that could be employed are the one by Egiazaroff (1965) or the correction of Egiazaroff (1965) by Ashida and Michiue (1971). The relation by Parker and Klingeman (1982) is chosen because it has a calibration factor that can be tuned for modelling of this experiments, contrary to the other formulations.

Both the prefactor A_{cal} (which is equal to 8 in the original relation) and the power A_{SKLHE} of the hiding and exposure relation are used for the calibration of the sediment transport. The prefactor A_{cal} was varied between 1 and 20 and the hiding exposure exponent parameter A_{SKLHE} ranged between 0.1 and 0.9. Both parameters within reasonable values lead to obtaining 180 simulations. These are first compared for the transport magnitude (cf. Figure 3.2)

In all simulations for the calibration the underlayer concept of (Hirano, 1971) is used, where the active layer L_{a} has a thickness of $\Delta/2$. In the case of the T5 simulation this results in an active layer thickness of 0.019 m. Setting the active-layer thickness to half the dune height is based on the idea that the upper boundary of the active layer (i.e, the bed level) must be at the mean bed elevation (i.e., half the dune height) and the lower end of the active layer is at the elevation of the dune troughs (i.e., half the dune height below the mean bed level) (Ribberink, 1987; Blom and Parker, 2004). This is a valid representation of the part of the bed that is mixed when bedform properties remain constant with time and are relatively regular. In field cases modelling long term development where dune height (and statistics) and mean bed elevation vary substantially, usually a larger value is necessary for capturing the right celerity of mixing changes. In this study, considering that a laboratory case is modelled, the assumption of half dune height seems plausible and reasonable. The bookkeeping layers all have a thickness of 0.01 m.

In the T5 experiment the coarsest fractions are immobile (Blom *et al.*, 2003, Figure 10.). This in combination with the total transport is used to calibrate the transport formula.

In Figure 3.3 the 10 simulations that better approximate the total load are compared to the measured composition of the transport. The simulation with A_{cal}=13 and A_{SKLHE}=0.9 may be the one that best performs in terms of fit to the data. However, a key property in modelling this experiments is that, as it was measured, the coarsest fractions are immobile under low flow conditions. For this reason, we select the simulation with A_{cal}=9 and A_{SKLHE}=0.7. This is accurate enough for modelling the total load and the load per size fraction and, most importantly, it correctly captures immobility of the coarsest fractions. It would be possible to calibrate the sediment transport rate of each size fraction individually for a perfect agreement. Still, the point of this exercise is not to perfectly reproduce the experiments but to show the consequences of modelling using the HANNEKE model.

Furthermore, it would be ideal to not only calibrate the sediment transport relation but also validate it against more data or morphodynamic development. Data is scarce for an extended validation and in this one-dimensional experiments no changes are predicted when using the active-layer model (Section 3.4). For this reason and without loss of generality, the calibrated formulation will be employed in the following steps.

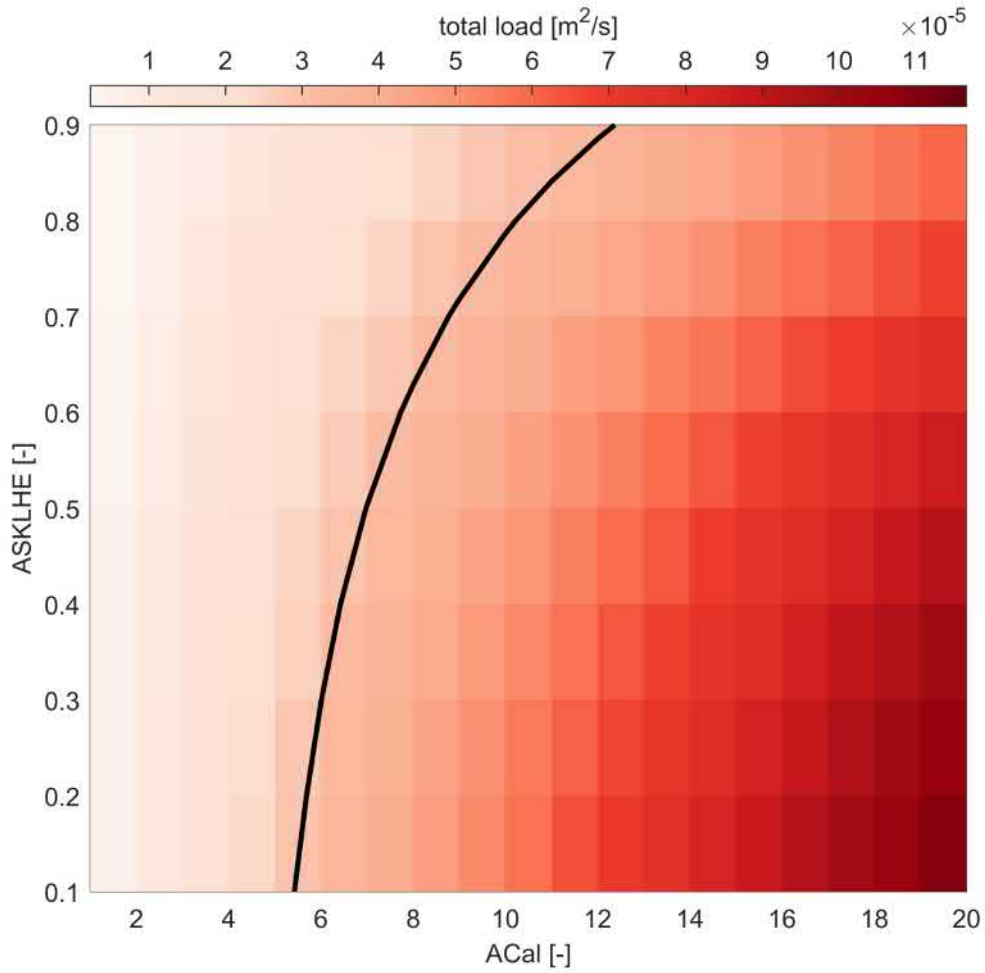

Figure 3.2 Total transport for various parameters of A_{cal} and A_{SKLHE}. The contour line denotes the measured transport per unit width for the T5 experiment.

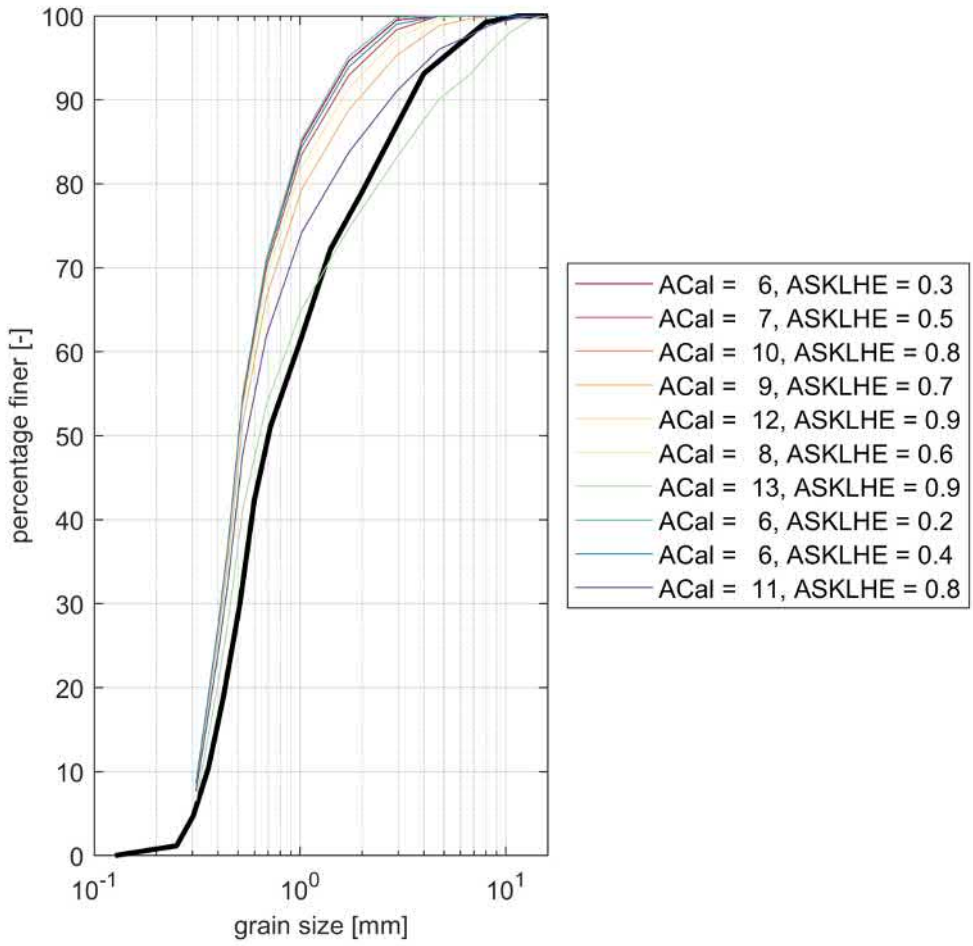

Figure 3.3 Composition of sediment load of T5 experiment for the 10 best performing with magnitude comparison. The black line denotes the measured composition.

3.3 Model setup

Having found the optimal coefficients for the sediment transport, the next steps are to model the evolution of the bed level and the subsurface. To this end, two model concepts are used of which the details can be found in (Chavarrías *et al.*, 2021). The first is the standard (Hirano, 1971) underlayer concept, and the second is the HANNEKE model in which a sorting of immobile sediment from the active layer into a coarse layer lying directly beneath it. An overview of the model concepts as applied in the modelling of the (Blom *et al.*, 2003) experiments is given below:

Model	L_a	L_c [mm]	Hiding-exposure
Hirano	$\Delta/2$	-	Active layer content
HANNEKE	$\Delta/2$	9.5	Combined active and coarse layer content

Table 3 Used model concepts for active layer and coarse layer thickness if present and for the computation the hiding and exposure correction.

3.4 Results

3.4.1 Sediment transport

The model was calibrated using the Hirano approach, and when applying the HANNEKE model, the transport distribution is rather similar to the calibrated Hirano approach (cf. Figure 3.4).

Using the HANNEKE model the coarse sediment is transferred to the coarse layer and the overall transport is slightly larger in magnitude. This is because, as coarse sediment is transferred to the coarse layer, the relative portion of sediment in transport (in the active layer) is altered compared to the Hirano approach. This results in a slightly higher, abut comparable, transport magnitude.

Although a separate calibration might be possible for each of the different models, the approach shows comparable behaviour. In reality measurements will not be as detailed as this experimental setup, and it is also useful for this and subsequent studies that the sediment transport formula in use is the same. After applying the different approaches to the T7 and T9 experiments, the transport of the HANNEKE model shows comparable transport magnitude to the Hirano approach (cf. Table 4). The transport for the T7 case is overestimated in comparison to the measured values. For the purpose of this study, which is to show the practical implication of the HANNEKE model in comparison to the Hirano model, the calibration suffices. As explained in Section 3.2, the essence is that fractions are correctly modelled as mobile or immobile depending on the flow and a difference in the magnitude of the transport is less relevant. The lack of fit to the data is not only because of the parameters of the calibrated sediment transport relation but also because the measured composition in T9 is different than in T5 while the modelled one is not.

3.4.2 Bed composition

The evolution of the bed composition is shown in Figure 3.5. The initial composition is shown in combination with the final equilibrium state. Neither in the active-layer nor in the HANNEKE model there are changes in streamwise direction. The experiments were conducted under normal flow conditions. As a consequence, the only fluxes of sediment are vertical. There are no waves propagating in the streamwise direction and the solution is the same at all locations.

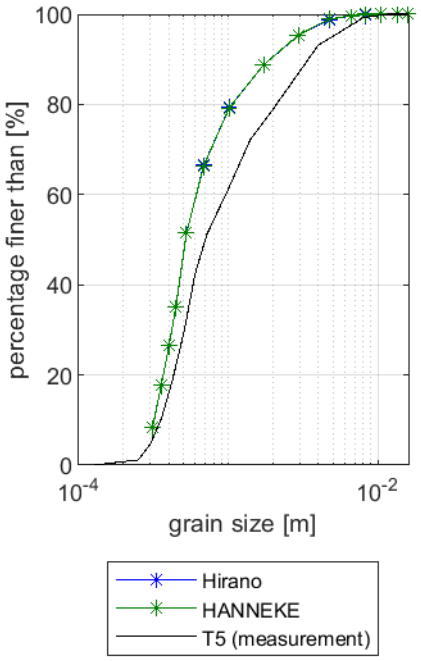

Figure 3.4 Transport for T5 for different methods.

Model / Measurement	Experiment		
	T5	T7	T9
Hirano	**3.23**	8.67	3.32
HANNEKE	3.49	8.69	3.56
Measurement	3.15	5.46	3.77

Table 4 Sediment load 10^{-5} [m^2/s] for varying models and as measured. In bold is the model which was used for the calibration

In the T5 simulations initially the sediment composition is uniform over the vertical. As the flow is in equilibrium and has a constant flow depth and velocity, using the Hirano model does not result in a change of the subsurface composition. When using the HANNEKE model the coarse layer develops and the coarse sediment is transferred from the active layer.

The T7 simulation starts from the end composition of T5. Again here a normal flow is imposed, and for this reason the initial condition is based on the subsurface composition of the HANNEKE model. Basing it on Hirano, would result in no variation over the vertical. Using the Hirano model as the active layer grows the subsurface becomes uniform over the vertical. The HANNEKE model shows a coarser active layer than in the T5 simulation as more fractions are now mobile. At the end of the T7 the active layer has mixed with the initial coarse layer. The variation of the active layer is minor at the end of the T7 experiment.

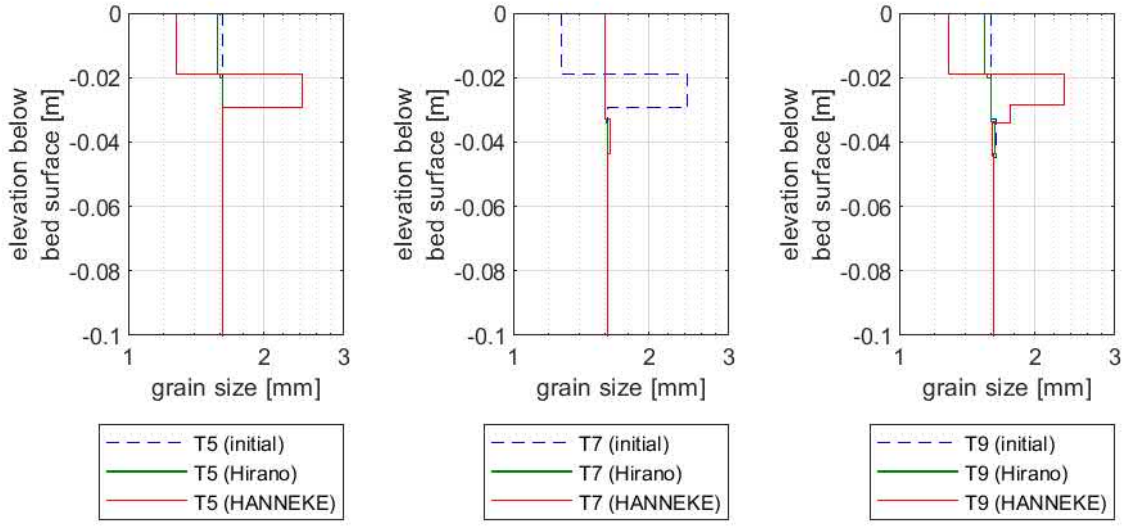

Figure 3.5 Sediment composition for different experiments for different models. In each case the initial composition is generated by the HANNEKE model

The T9 simulation starts again from the T7 HANNEKE result. If a Hirano approach had been used throughout (T5 through T9) no variation in the subsurface would be found. The Hirano model does not show a difference from the initial T9 situation, as the active layer thickness is now reduced compared to the T7 situation. The T9 HANNEKE simulation shows a coarse layer which is lower than in the T5 situation, after the passage of the flood conditions. This indicates that some memory of the flood can be captured using the additional sorting flux in the underlayer model. In the subsequent chapters the relative influence of different terms will be simulated and discussed.

The comparison to the measured values is in theory possible from Figure 3.6, but this is a qualitative assesement of the HANNEKE model and refining these choices and the transport could improve the result quantitatively as well, but is sufficient to show the principles of the model.

The measurements show that when sampling in the troughs the sediment is coarser than the same location when sampling at the crest. This can be attributed to the winnowing of fines from the coarse layer. This behaviour is not captured in the HANNEKE model or the Hirano model. The measurements of T7 show a layer of coarse sediment at the trough elevations which is not captured by neither the HANNEKE nor the Hirano model. The Hirano model is not capable of capturing the coarse-layer formation in any case and the HANNEKE model does not predict the presence of the coarse layer because for this discharge all sediment is mobile.

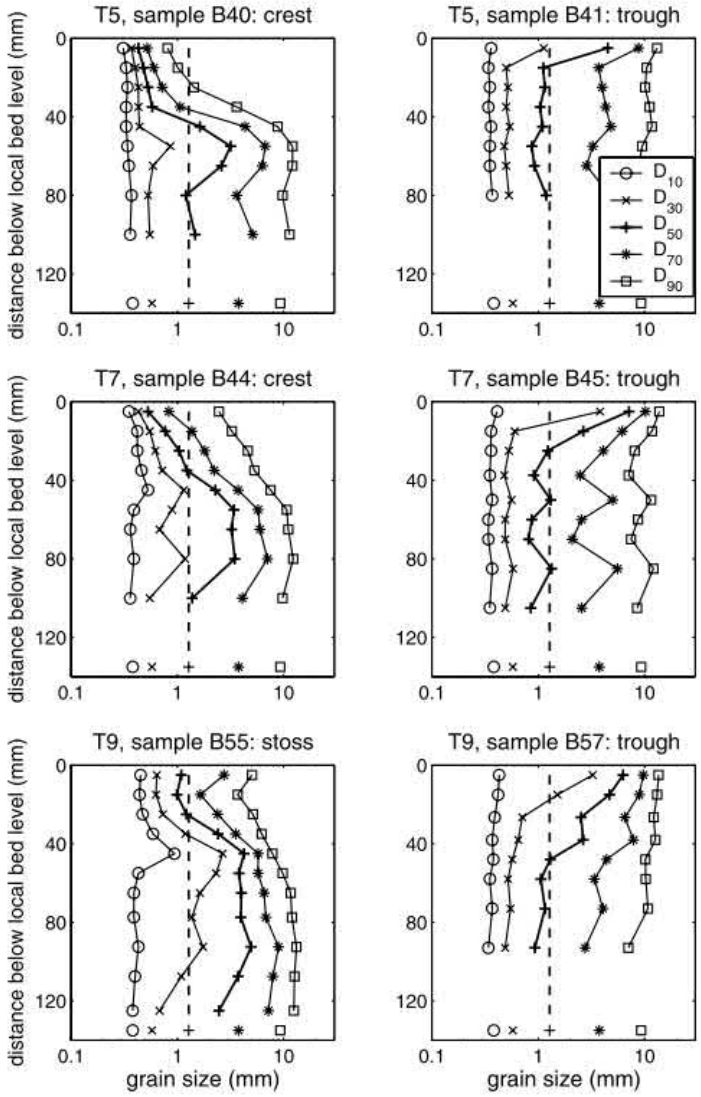

Figure 3.6 Core samples taken at crests and in troughs in experiments T5, T7, and T9 (Rhine mixture): variation of D10, D30, D50, D70, and D90 over depth (see legend in top right plot) compared with D10, D30, D50, D70, and D90 of the original mixture (see symbols at bottom of each plot). The D50 of the original mixture is also indicated by the vertical dashed line (from Blom *et al.* (2003)).

4 1D idealized field case

In this section the models are applied to an idealized field case for studying the effects and consequences of the different modelling and parameter choices.

4.1 Simulation set-up

A schematized one-dimensional domain inspired in the Waal is considered. The domain is 100 km long. A single half-sinus flood wave with a period T =50 days is imposed (Figure 4.7) preceded and succeeded by 50 days-long periods of low flow. Considering a width equal to 280 m, the discharge varies between 1000 m^3/s and 6000 m^3/s. A Chézy friction type is employed with parameter 37 $m^{1/2}/s$. The initial bed is flat with a constant slope equal to 1×10^{-4}. This yields a normal flow depth for the limit discharges equal to 4.53 m and 14.97 m, respectively. At the downstream end the water level is fixed at 10 m. In this way, a backwater curve will be present that creates streamwise changes.

The sediment is discretized into 5 size fractions with the sizes specified in Table 5. Initially, the bed surface and substrate is composed of 20% of each size fraction (i.e., equally distributed). Sediment transport is modelled using the relation by Meyer-Peter and Müller (1948) (Equation ((3.1))) with the power-law hiding exposure by Parker *et al.* (1982) with parameter 0.7 (Equation ((3.2)). The sediment in the coarse layer is not involved in computing the hiding-exposure effect. The alluvial active-layer thickness is set proportional to the square root of flow depth with a factor $\alpha_{\mathrm{L}} = 0.3$:

$$L_{\mathrm{a}} = \alpha_{\mathrm{L}} \sqrt{H} \ . \tag{4.1}$$

Van Rijn (1984) proposes a relation varying with a power 0.7 of the flow depth. Here a power 0.5 is employed for limiting the variation of the active-layer thickness to reasonable values given the large changes in flow depth. Similarly, factor α_{L} is chosen for obtaining reasonable values given the conditions of the idealized case. The minimum thickness of the active layer is set to 0.5 m. The coarse layer is set to a constant equal to L_{c} =0.5 m. The substrate is discretized using 0.1 m thick layers.

fraction	characteristic grain size d_k [m]
1	0.0005
2	0.001
3	0.004
4	0.008
5	0.016

Table 5 Characteristic grain sizes of the reference simulation.

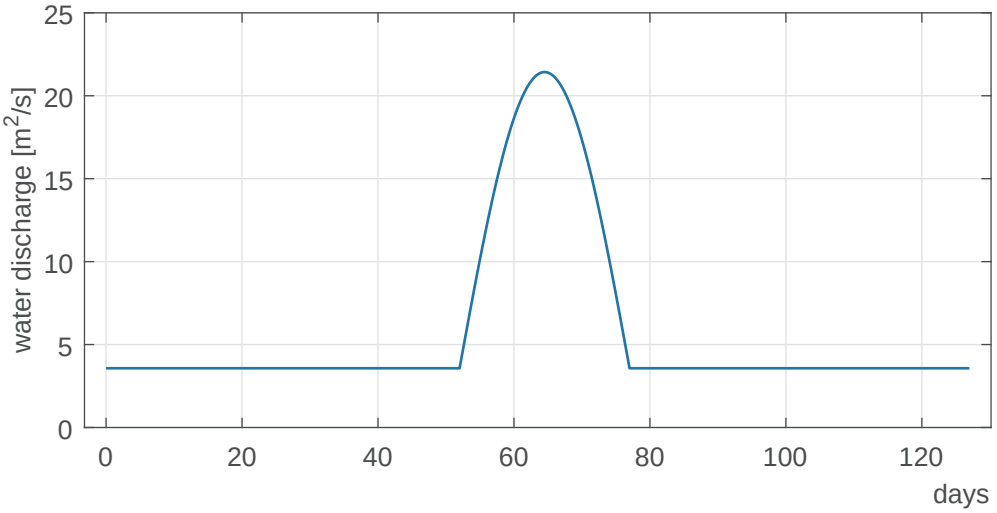

Figure 4.7 Reference flood wave.

The timescale of the sediment flux from the active layer to the coarse layer is (Chavarrías *et al.*, 2020):

$$T_{\mathrm{imm}} = \frac{L_{\mathrm{a}} \Lambda_{\mathrm{cl}}}{q_{\mathrm{b}}} \ , \tag{4.2}$$

where Λ_{cl} is average length between the dune troughs which reach the coarse layer which is equal to:

$$\Lambda_{\mathrm{cl}} = \alpha_{\Lambda} \Lambda \tag{4.3}$$

where Λ [m] is the average dune length under alluvial conditions and α_{Λ} [-] is a parameter for considering the effect of the coarse layer in estimating the dune length:

$$\alpha_{\Lambda} = 1 + (\alpha_{\mathrm{m}} - 1) \frac{L_{\mathrm{a}}}{L_{\mathrm{a0}}} \ , \tag{4.4}$$

where $\alpha_{\mathrm{m}} \geq 1$ [-] is the maximum value of α_{Λ} (reached when $L_{\mathrm{a}} = L_{\mathrm{a0}}$). Parameter α_{m} is set to 1.

The bed level and composition are fixed at the upstream end. A spin-up period of 2 days is used, such that hydrodynamics are stable before morphodynamic changes start.

4.2 Parameter space

The reference simulation is run using the active layer and HANNEKE models. Key parameters controlling the timescale of mixing in the HANNEKE model are the alluvial active-layer thickness (controlled by α_{L}), the coarse-layer thickness, and the parameter relating the dune length to the timescale of immobile-sediment deposition (i.e., α_{m}). Nine simulations are run combining double and half the active-layer thickness and coarse-layer thickness. One simulation is run in which α_{m} is 10 times smaller than in the reference case (i.e., immobile sediment depositions occurs 10 times faster). Table 6 summarizes all variations.

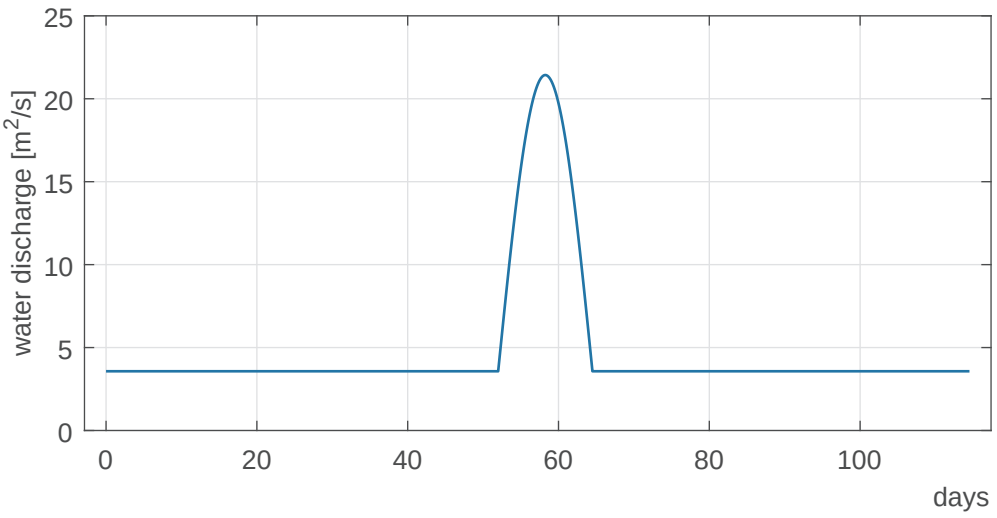

Figure 4.8 Flood wave with half period.

The number of sediment size fractions in which the mixture is discretized is crucial. The main property of the HANNEKE model is that immobile sediment is transferred to the coarse layer underneath the active layer. Hence, whether a sediment size fraction is mobile or not is of utmost importance. Using an increasing number of size fractions usually implies that the range of characteristic grain sizes increases. Hence, when increasing the number of characteristic grain sizes a certain amount of sediment will be represented by a coarser grain size which may be immobile. To study this effect we run a simulation with the same mixture as the original one but discretized using 2 sediment size fractions. The 4 coarsest size fractions are lumped in a single fraction with an equivalent characteristic grain size equal to d_2 =4.7568 mm obtained as the geometric mean:

$$d_2 = 2^{\sum_{k=2}^{N} \frac{1}{4} \log_2 d_k} \ , \tag{4.5}$$

where N is the number of size fractions.

The flood wave period has an influence on the mixing scale given that the timescale of immobile sediment deposition depends on the sediment transport rate and the active-layer thickness. For testing this, a simulation equal to the reference except for the fact that period of the flood wave is halved is conducted. This is controlled by parameter $\alpha_T = T_\mathrm{r}/T$ [-], which is the ration between the period of the reference simulation and the period of the particular simulation (Table 6).

#	α_{L} [-]	L_{c} [m]	N [-]	α_T [-]	α_{m} [-]	legend
00	0.30	0.50	5	1	1.0	Hirano
01	0.30	0.50	5	1	1.0	$\alpha_L = 0.30$, $L_c = 0.50$ m
02	0.30	0.25	5	1	1.0	$\alpha_L = 0.30$, $L_c = 0.25$ m
03	0.30	1.00	5	1	1.0	$\alpha_L = 0.30$, $L_c = 1.00$ m
04	0.15	0.50	5	1	1.0	$\alpha_L = 0.15$, $L_c = 0.50$ m
05	0.15	0.25	5	1	1.0	$\alpha_L = 0.15$, $L_c = 0.25$ m
06	0.15	1.00	5	1	1.0	$\alpha_L = 0.15$, $L_c = 1.00$ m
07	0.60	0.50	5	1	1.0	$\alpha_L = 0.60$, $L_c = 0.50$ m
08	0.60	0.25	5	1	1.0	$\alpha_L = 0.60$, $L_c = 0.25$ m
09	0.60	1.00	5	1	1.0	$\alpha_L = 0.60$, $L_c = 1.00$ m
10	0.30	0.50	2	1	1.0	$N = 2$
11	0.30	0.50	5	2	1.0	$\alpha_T = 2$
12	0.30	0.50	5	1	0.1	$\alpha_m = 0.1$

Table 6 Idealized one-dimensional simulations. In the legend, only the values different from the reference situation are mentioned.

4.3 Results

4.3.1 Reference case

The initial condition is the same for all cases in terms of mean grain size at the bed surface. Figure 4.9 present a longitudinal profile of the mean grain size. During the low flow period before the flood wave there is an M1 backwater curve along the model causing a decreasing sediment transport capacity in streamwise direction. This causes that Fractions 4 and 5 are immobile along the whole river but Fraction 3 is mobile only until x =35 km approximately being x the streamwise coordinate (Figure 4.10). Fractions 1 and 2 are mobile along the whole domain. As a consequence, the coarse layer up to x =35 km right before the flood wave is coarser than from x =35 km onwards. It may seem counter-intuitive that the coarse layer is finer under lower flow conditions but it is correct and logical. In the upstream reach the coarse layer is formed only by Fractions 4 and 5 while downstream is formed by 3, 4, and 5, which yields a finer average. The situation at this point is not in equilibrium. As a sediment size fraction becomes immobile in the domain, equilibrium would only be achieved when the river bed has aggraded such that the coarse fraction entering the model upstream reach the downstream end. This end result would be achieved in the order of decades and is of little relevance for understanding the implications of the model parameters.

In the active layer we observe that it is slightly finer from x =35 km onwards. This is explained from the fact that it is only composed of Fractions 1 and 2 rather than 1, 2, and 3, as it happens upstream from x =35 km. Noticeably, the active-layer thickness is thinner from x =35 km onwards. This is because Fraction 3 is transferred from the active layer to the coarse layer but there is no mobile material in the coarse layer to replace it. The slight erosion observed at the transition point is explained by the sudden decrease in sediment transport rate at the point as Fraction 3 becomes immobile.

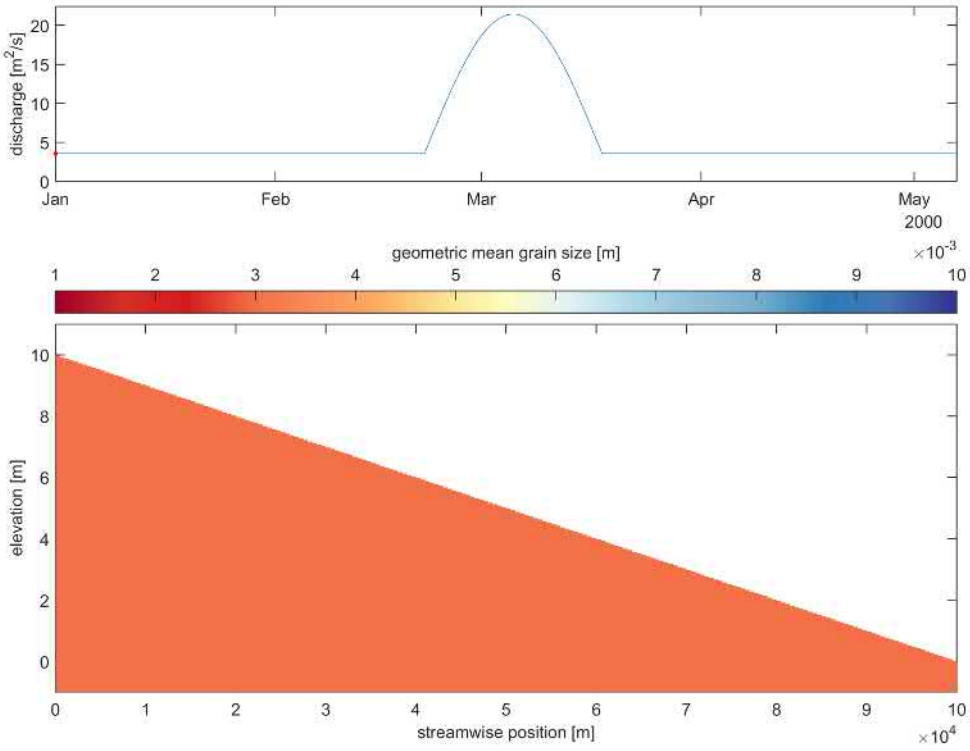

Figure 4.9 Longitudinal profile of the mean grain size at the start of the run 01.

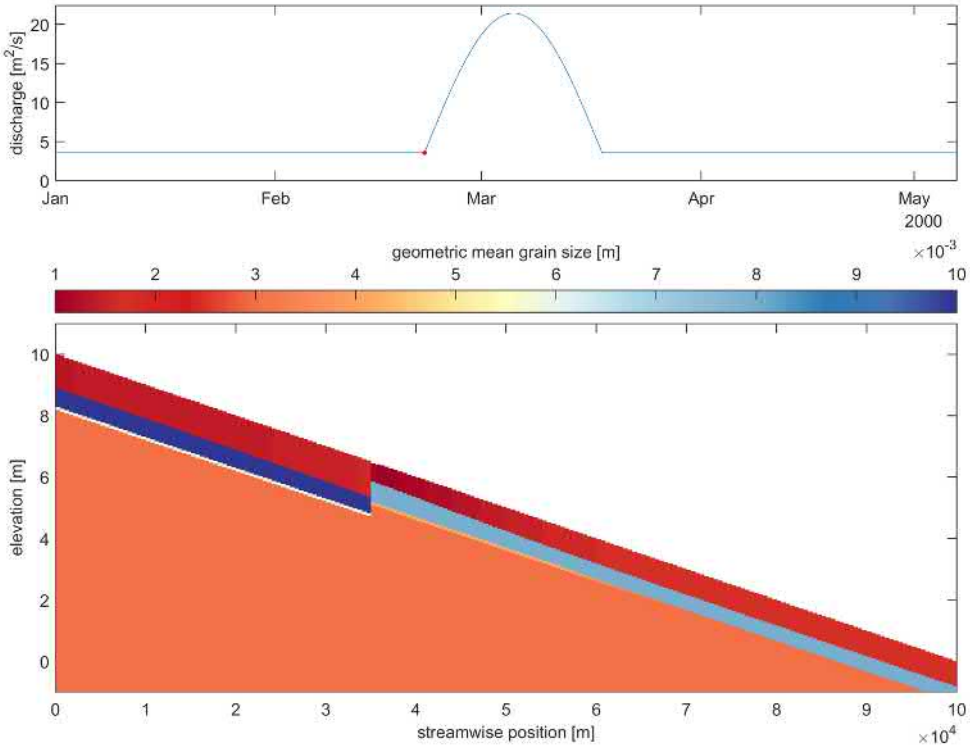

Figure 4.10 Longitudinal profile of the mean grain size before the flood wave in run 01.

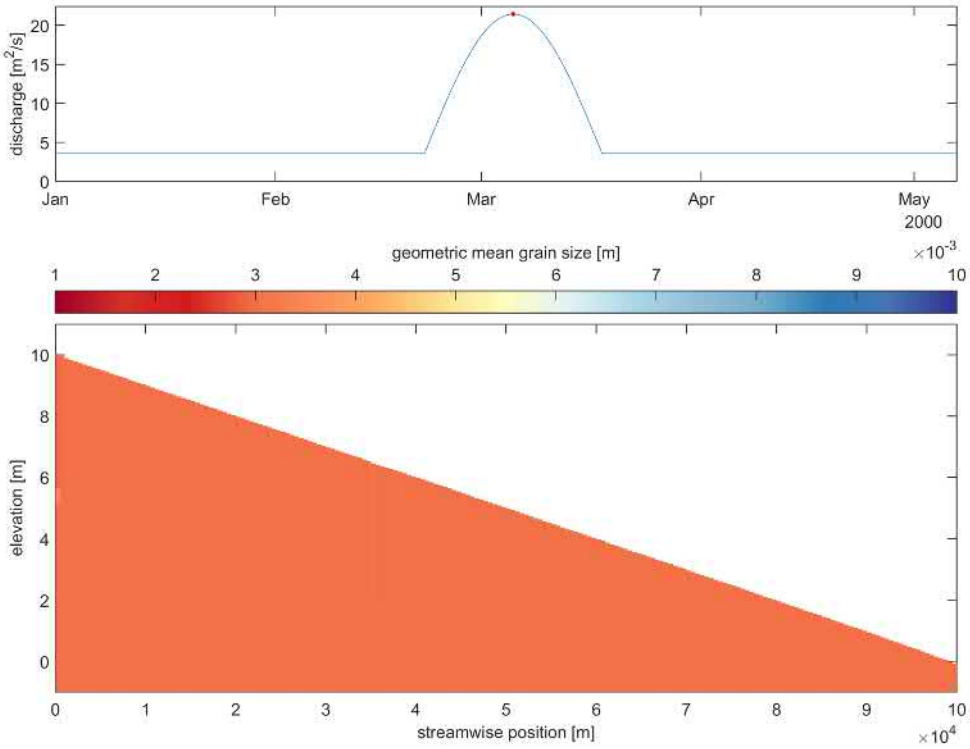

Figure 4.11 Longitudinal profile of the mean grain size at the flood wave peak in run 01.

At the peak of the flood wave all sediment is mobile and entrained (Figure 4.11). Hence, there is no stratification. As the flood wave recedes, some size fraction start becoming immobile and being transferred to the coarse layer (Figure 4.12). Eventually, the river shows the profile in Figure 4.13.

Comparing the final profile after a period of low flow with the profile before the flood wave (also after a period of low flow), a striking result is that at the end, the active layer thickness substantially increases in streamwise direction, and no hard transition is found at x =35 km. The reason that explains the larger active layer thickness at the end of the run is that the flux of sediment to the coarse layer depends on the sediment transport rate. Due to the M1 backwater curve, the sediment transport rate decreases in streamwise direction and the transfer of sediment out of active layer slows down. A coarsening in streamwise direction is observed due to the same mechanism. This result is, again, realistic. A small amount of sediment transport after a flood event will not be able to rework the sediment and transfer coarse sediment below via lee-face sorting mechanisms.

The model predicts a band of coarse sediment (between z =5 m and z =7 m approximately at x=0, being z the vertical coordinate). This is due to the fact that when the coarse layer was at that elevation, the coarsest fractions were immobile and transferred to the coarse layer. As the coarse layer moved upward when the active layer became thinner, the coarse sediment was transferred to the substrate.

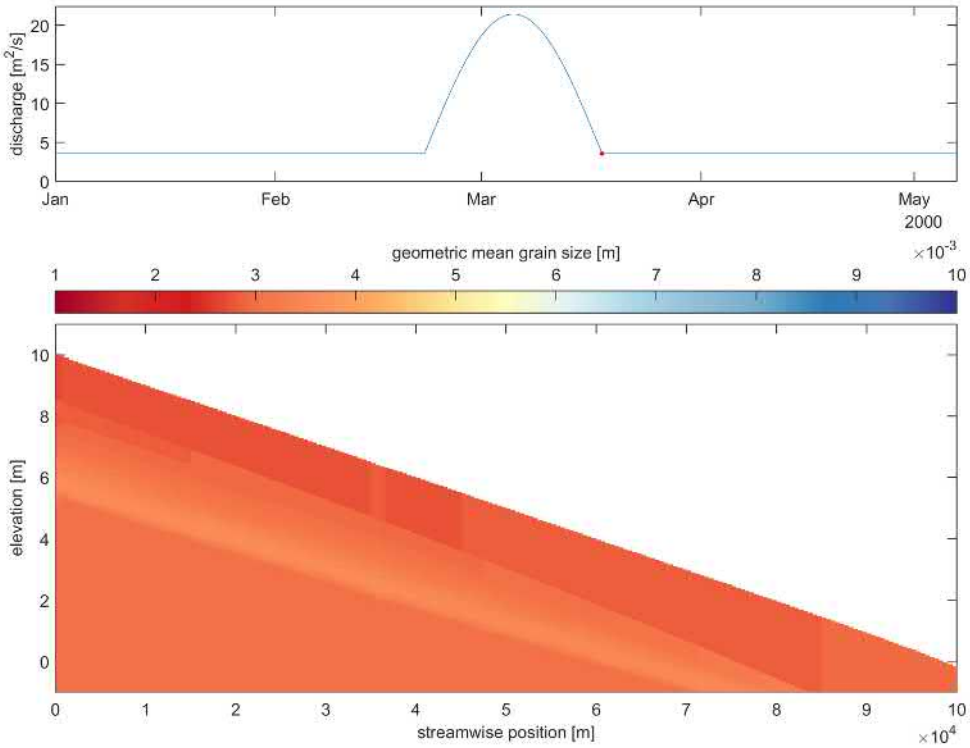

Figure 4.12 Longitudinal profile of the mean grain size after the flood wave peak in run 01.

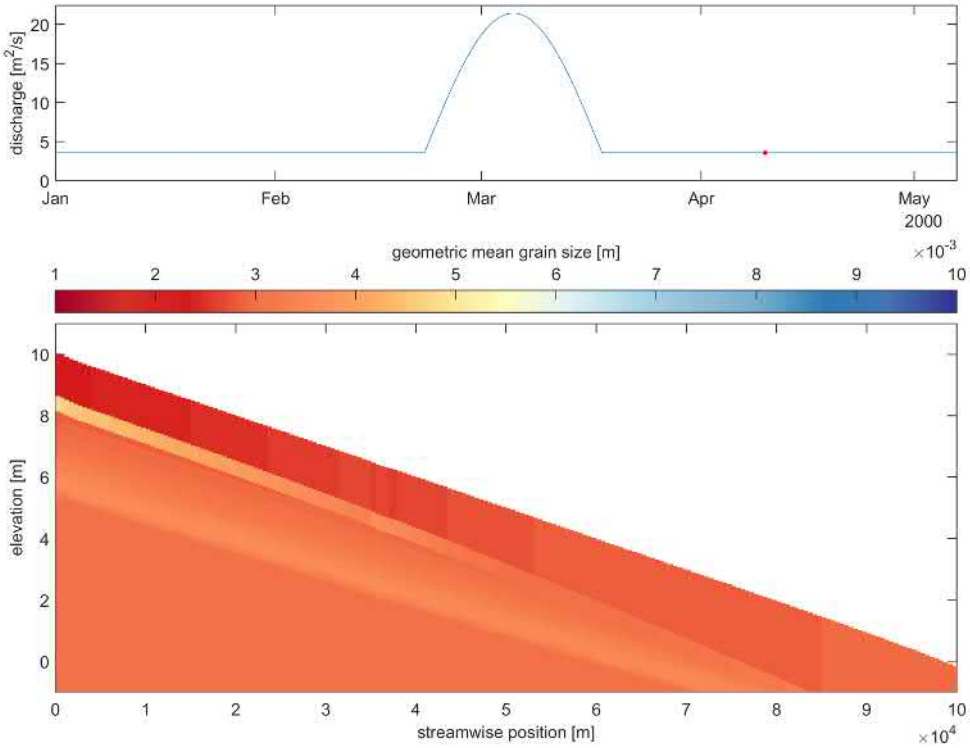

Figure 4.13 Longitudinal profile of the mean grain size at the end of run 01.

4.3.2 Active-layer model

Contrary to the HANNEKE model, the active-layer model predicts negligible changes in sediment composition for the whole simulation period (e.g., Figure 4.14). Figure 4.15 shows the same information using a colour scale specific to highlight the minimal changes. The reason for this is that in the active-layer model vertical sorting is only due to changes in mean bed elevation. Although a flood wave passes and there is a backwater curve, the changes in mean bed elevation are not significant and hence there is no appreciable change in composition. Although the active layer increases in thickness during the flood wave, the sediment that is entrained has the same composition as the sediment available in the active layer. Similarly, as the active-layer thickness decreases, the sediment transferred to the substrate has the same composition as the one in the active layer and no stratification arises.

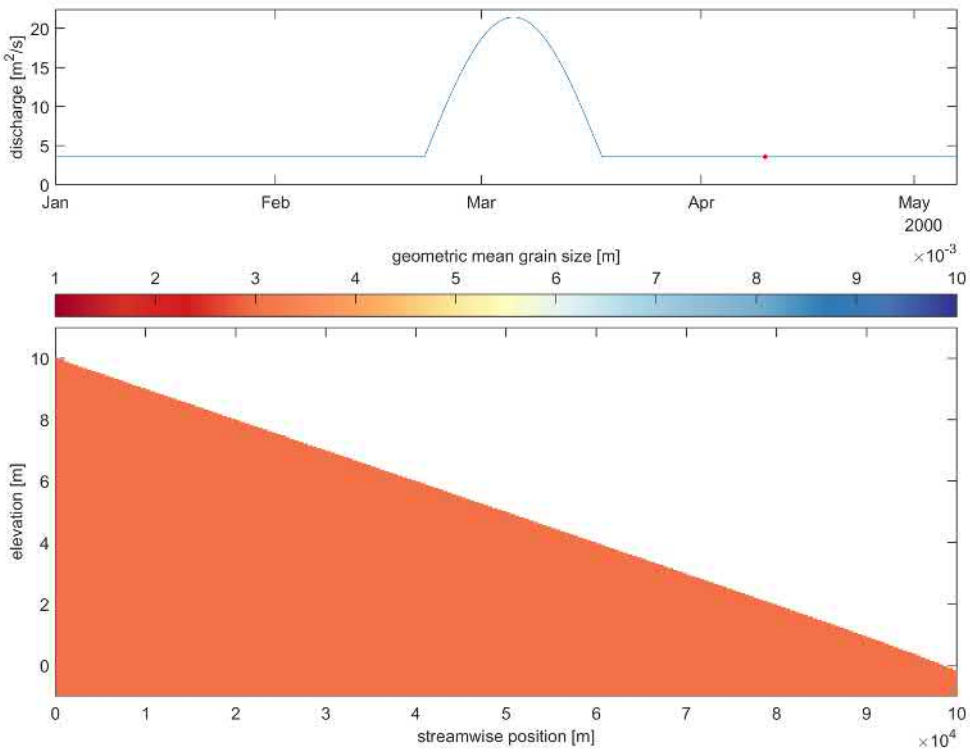

Figure 4.14 Longitudinal profile of the mean grain size at the end of run 00.

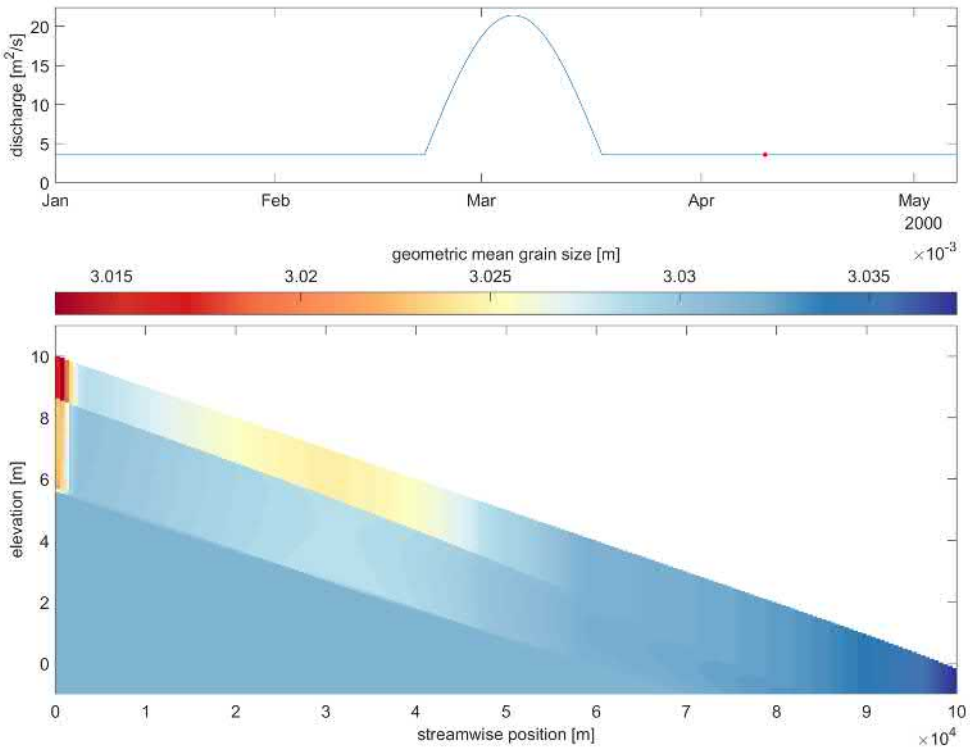

Figure 4.15 Longitudinal profile of the mean grain size at the end of run 00 using a colour scale specific for this case.

4.3.3 Active-layer thickness variation

An increase of the alluvial active-layer thickness has no effect in the situation before the flood wave (Figure 4.16). This is because the active-layer thickness at this stage is not limited by the alluvial value but by the availability of mobile sediment in the coarse layer.

On the other hand, a decrease of the alluvial value with respect to the reference value causes the coarse layer to be finer (Figures 4.17). In this case, the active layer thickness is limited by the alluvial value. As the coarse layer has the same thickness as in the reference case, the relative thickness of (i.e., also relative amount of sediment in) the active layer with respect to the coarse layer decreases. Hence, there is less amount of immobile sediment in the active layer and the coarse layer does not form completely. There is still mobile sediment in the coarse layer which is not transferred to the active layer because there is no more immobile sediment in the active layer being deposited.

There is also a large difference in the situation at the peak of the flood wave. The case with a large-active layer thickness (Figure 4.18) shows the same results as the reference case. On the other hand, a smaller active-layer thickness causes the coarse layer to be visible in the longitudinal profile (Figure 4.19). The reason is similar to the previous case. While the coarse sediment in the coarse layer is mobile and could be entrained into the active layer, this only occurs if the active layer has not reached its alluvial value. In this case it would be more appropriate to speak about a coarse top substrate layer rather than of a coarse layer, as this is not limiting transport in the active layer.

The same features as in the reference case are observed at the end of the run in both variations of the active-layer thickness with the difference that in the case that the active layer is thinner, the coarse band of sediment in the substrate is at a higher elevation because the thickness of sediment reworked has been smaller (Figures 4.20 and 4.21).

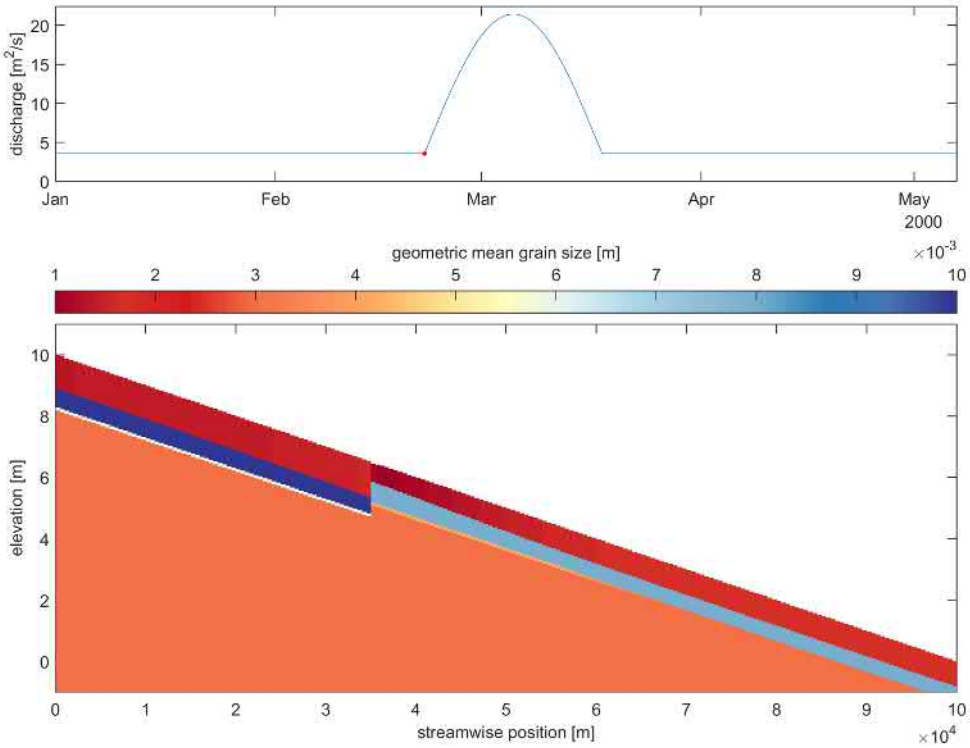

Figure 4.16 Longitudinal profile of the mean grain size before the flood wave in run 07.

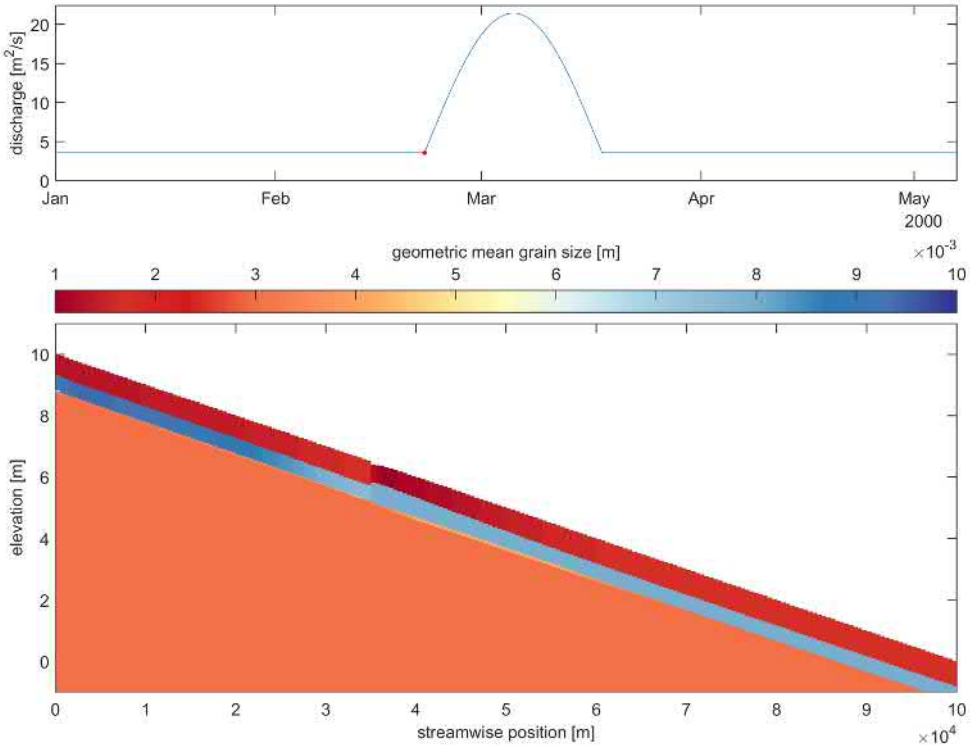

Figure 4.17 Longitudinal profile of the mean grain size before the flood wave in run 04.

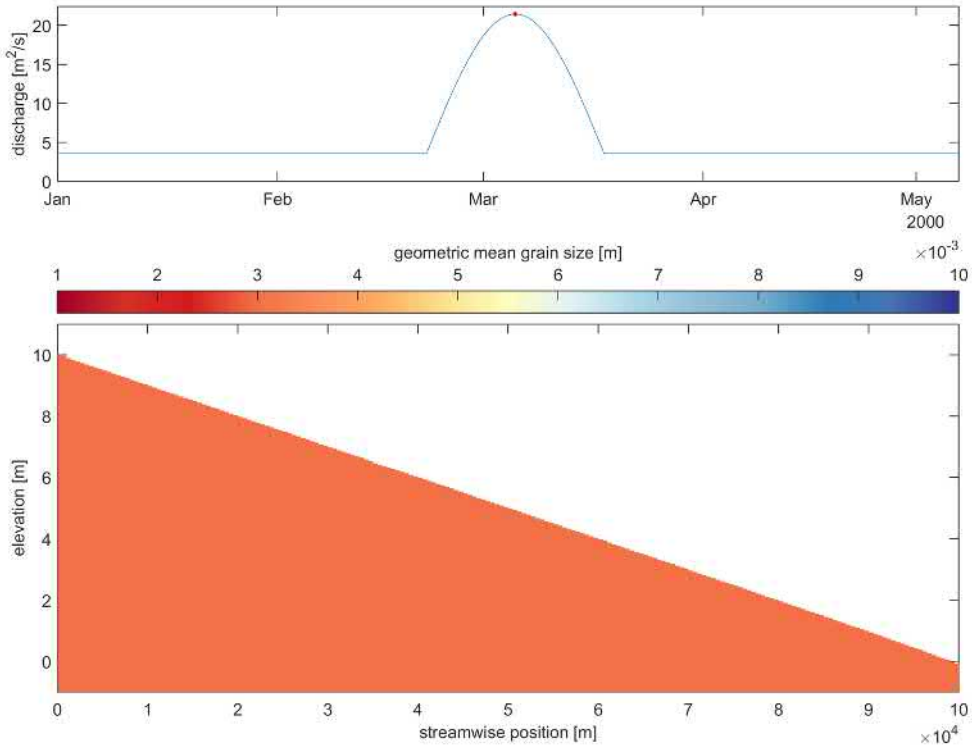

Figure 4.18 Longitudinal profile of the mean grain size at the flood wave peak in run 07.

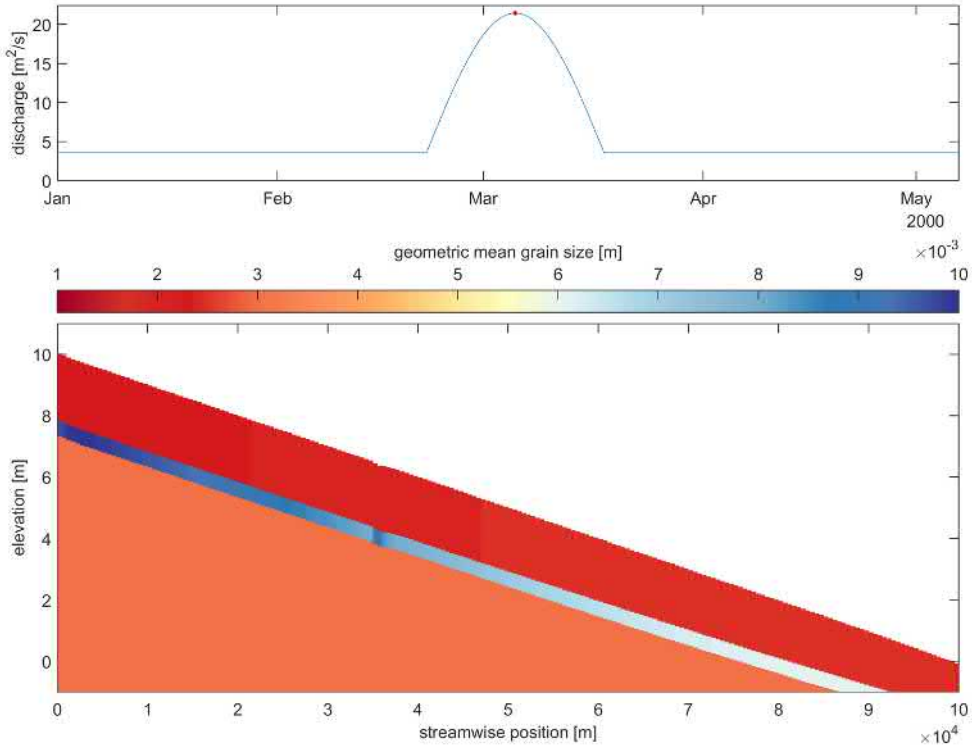

Figure 4.19 Longitudinal profile of the mean grain size at the flood wave peak in run 04.

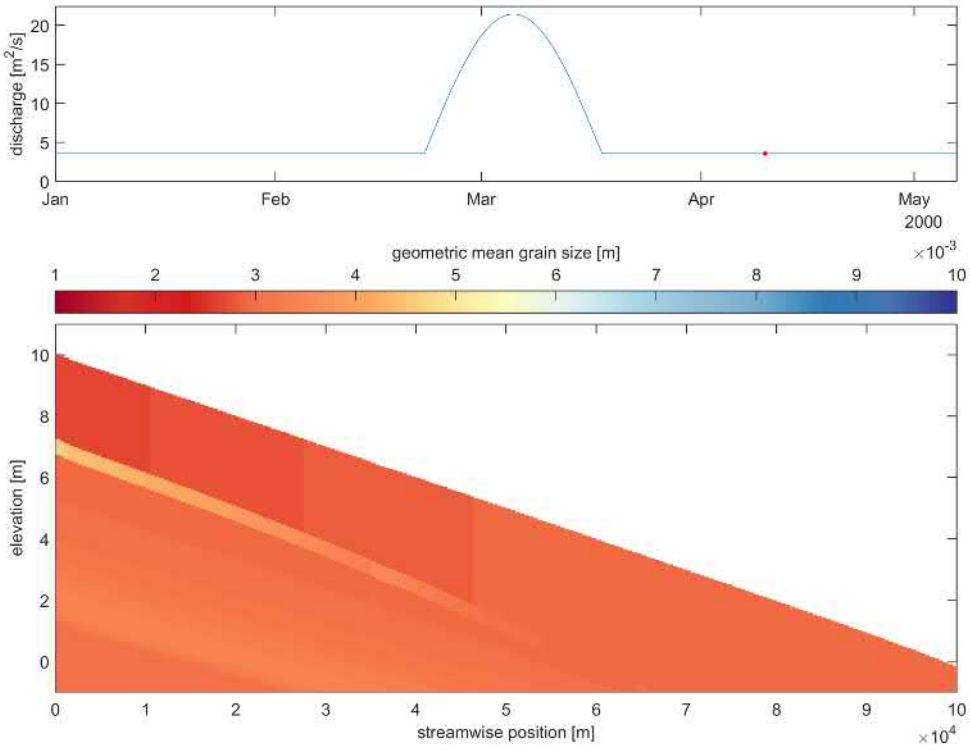

Figure 4.20 Longitudinal profile of the mean grain size at the end of run 07.

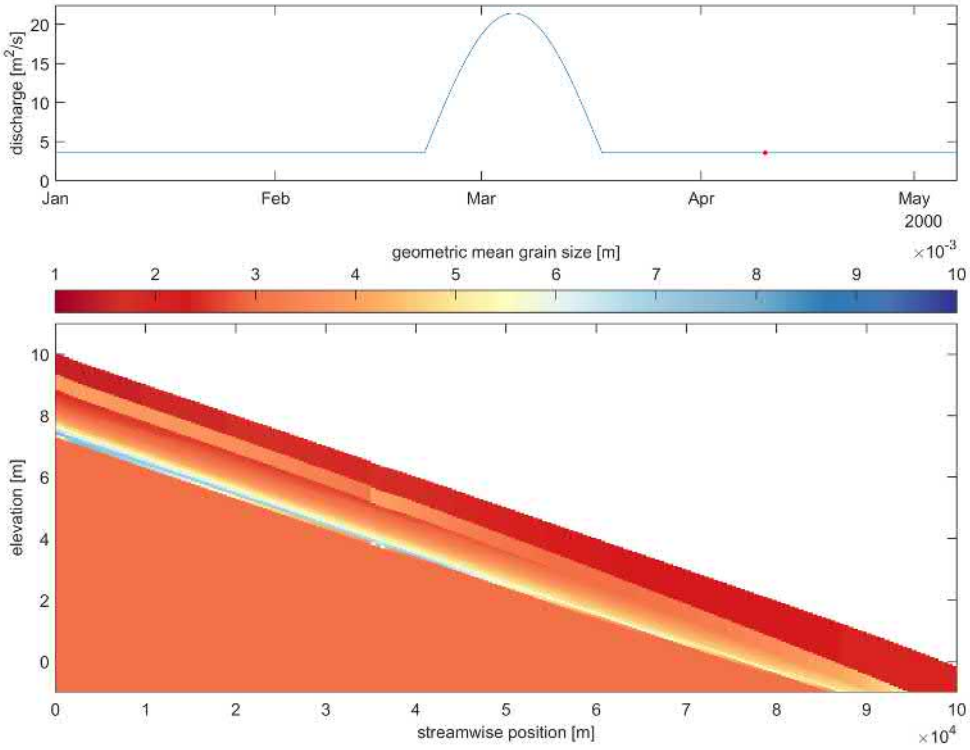

Figure 4.21 Longitudinal profile of the mean grain size at the end of run 04.

4.3.4 Coarse-layer thickness variation

Simulations 02 and 03 consider a thinner and thicker coarse layer compared to the reference case, respectively. After the first period of low flow, a thinner coarse layer causes a thinner active layer (Figure 4.22). Immobile sediment initially found in the active layer deposits into the coarse layer, which at the same time provides mobile material to the active layer. A thinner coarse layer implies that there is relatively less sediment in it. As a consequence, there is also less mobile sediment to be transferred to the active layer. The coarse layer becomes fully immobile earlier than in the reference case and the active layer stops growing.

The opposite occurs if the coarse-layer thickness is thicker (Figure 4.23). Relatively, more mobile sediment is initially in the coarse layer, which is transferred to the active layer as immobile sediment in the active layer moves down. In this case, the active-layer thickness achieves its alluvial value. This is seen not only from the fact that active layer is thicker than in the reference case, but also from the fact that the coarse layer is finer, as it still has mobile material that could be transferred.

A decrease in the coarse-layer thickness has no significant impact in the stratigraphy at the peak of the flood wave (Figure 4.24). The coarsest fraction becomes mobile and it transferred to the active layer as it increases in thickness. The same mechanism as in the reference case is observed. The coarse layer is fully formed before the flood wave, limiting the active-layer thickness. As the flow is able to mobile the sediment in the coarse layer, this is transferred to the active layer, which increases in thickness instantaneously given that it is below its alluvial value.

On the other hand, an increase in the coarse-layer thickness causes this to be visible during the peak of the flood wave (Figure 4.25). In this case, the active-layer thickness is not initially limited by the coarse layer being fully formed. During the rising stage of the flood wave the active layer increases in thickness always being able to reach its alluvial value. The coarse layer becomes coarser but not completely immobile. In the final stage of the rising, the coarsest fraction in the coarse layer becomes mobile and a part of it is transferred to the active layer but the active layer achieves its alluvial value while there is still coarse sediment underneath. Equally to the previous, in this case, the coarse layer behaves simply as a coarse top substrate layer.

The previous mechanism causes a different stratigraphy at the end of the run. A large amount of coarse sediment marks the maximum extent of the active layer when the coarse layer is thick (Figure 4.26). The coarse top substrate layer remains where it was at the peak of the flood wave. As the flood wave receded, the coarsest sediment size fractions become immobile and are transferred to the coarse layer. A decreasing active layer thickness causes the coarse layer to move upwards, which causes a transfer of coarse sediment to the substrate. This causes the layers of coarse sediment on top of the much coarser lowermost layer.

When the coarse layer is thin there is no coarse top substrate layer and the stratification is only due to the mechanism explained above (Figure 4.27). A thinner coarse layer again allows for a faster coarsening in the low flow period, clearly visible in the upstream end of the domain.

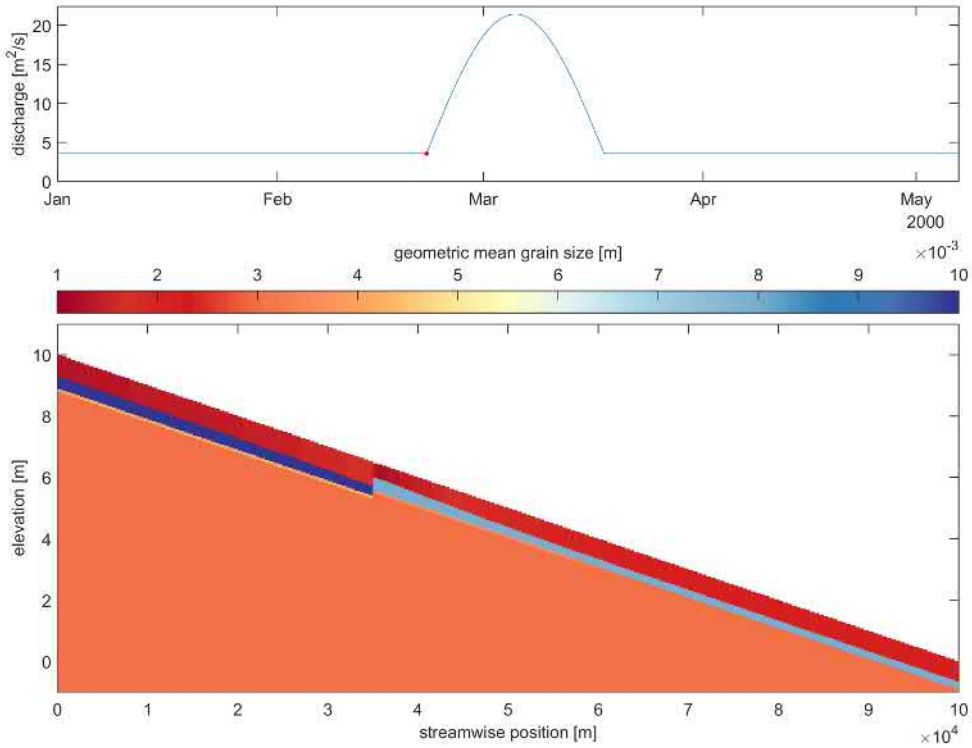

Figure 4.22 Longitudinal profile of the mean grain size before the flood wave in run 02.

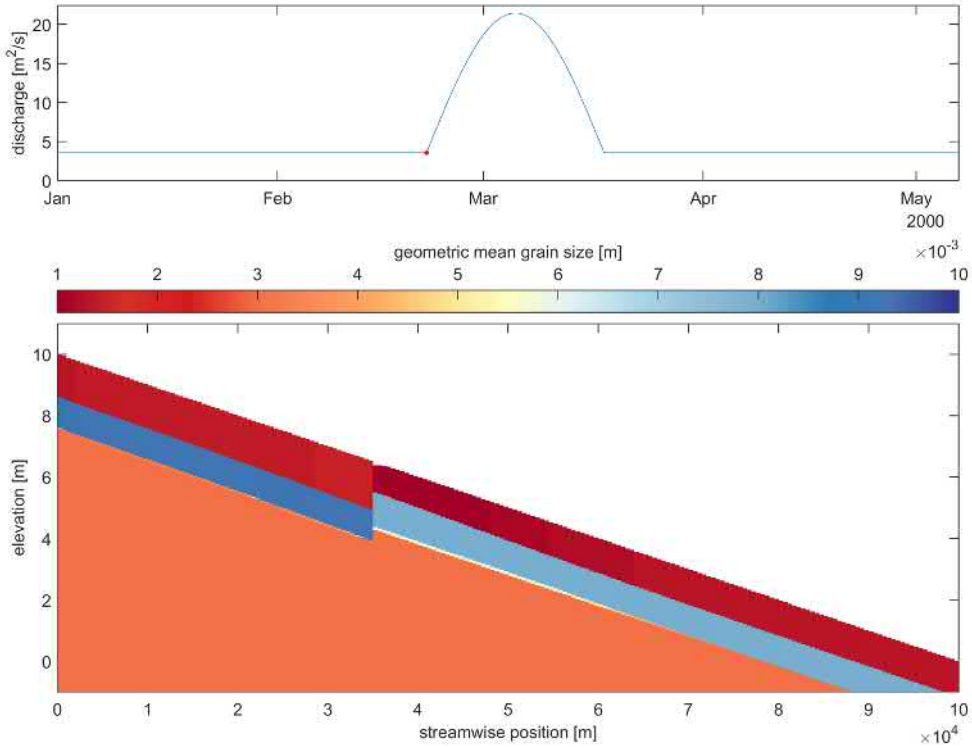

Figure 4.23 Longitudinal profile of the mean grain size before the flood wave in run 03.

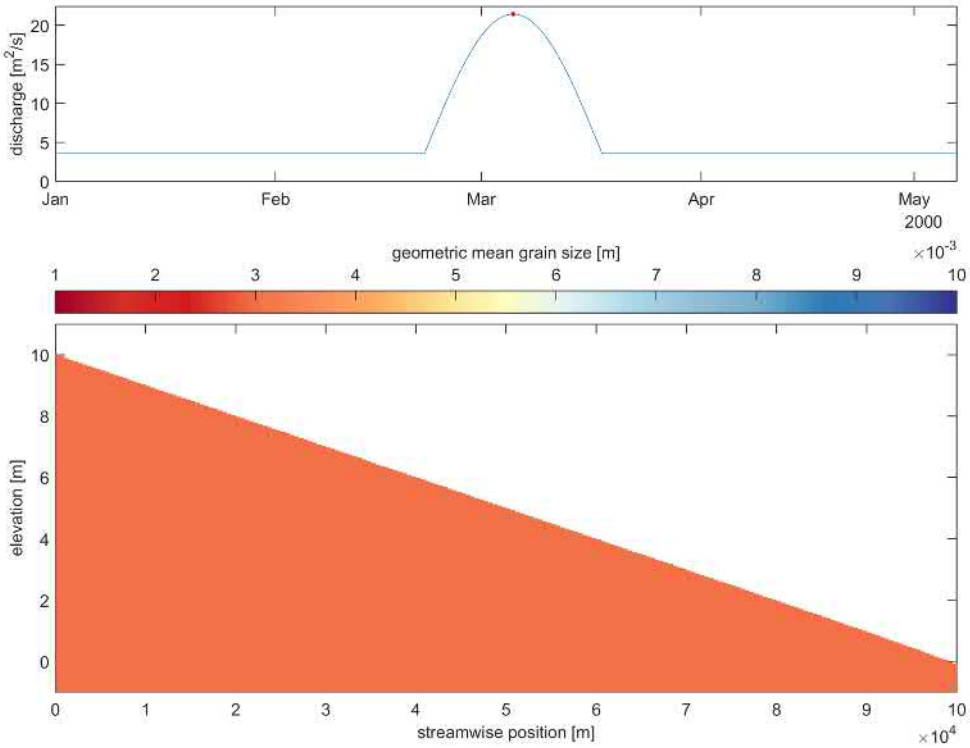

Figure 4.24 Longitudinal profile of the mean grain size at the flood wave peak in run 02.

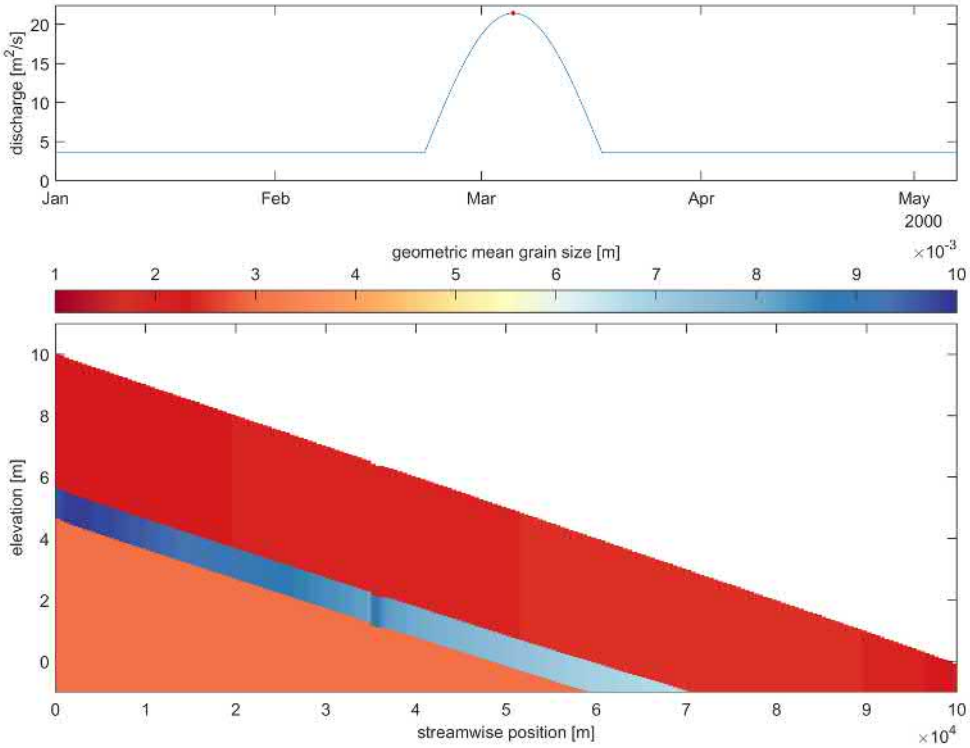

Figure 4.25 Longitudinal profile of the mean grain size at the flood wave peak in run 03.

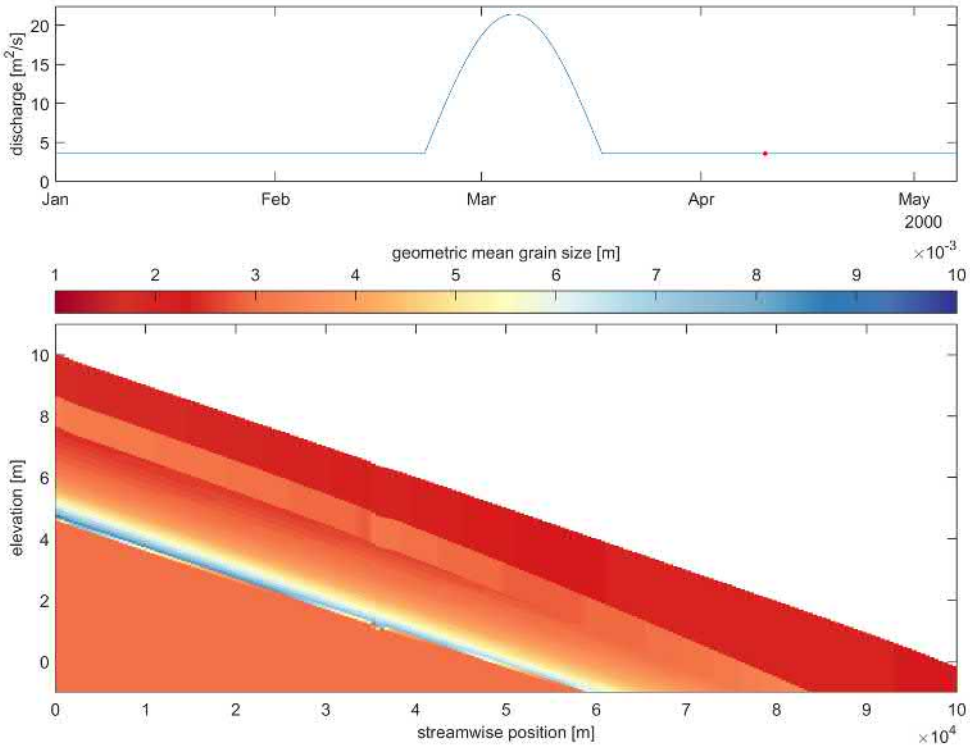

Figure 4.26 Longitudinal profile of the mean grain size at the end of run 03.

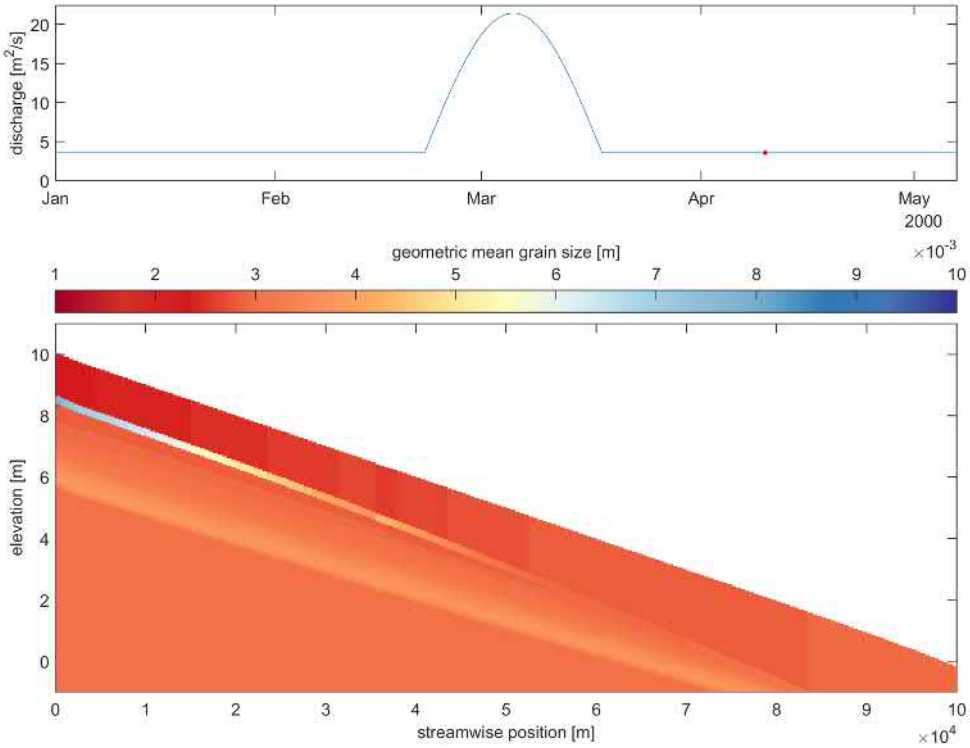

Figure 4.27 Longitudinal profile of the mean grain size at the end of run 02.

4.3.5 Proportional variation of the layer thicknesses

Simulations 05 and 09 model a proportional decrease and increase in active-layer and coarse-layer thickness. The same grain size distribution as in the reference case is found in both cases (Figures 4.28 and 4.29). When the active layer is thinner, less immobile sediment is available for being transferred from the active layer to the coarse layer. At the same time, the fact that the coarse layer is also thinner implies that the same amount of immobile sediment deposited causes a larger change in grain size distribution. The proportions of the layers being kept constant causes no overall effect in the grain size. The same happens at the peak of the flood wave.

The situation is different at the end of the run. The case with thinner layers (Figure 4.30) shows a larger degree of coarse-layer formation than the case with thick layers (Figure 4.31). Although the relative amount of sediment is constant, the timescale of immobile sediment deposition depends on the absolute value of the active-layer thickness (Equation (4.2)). The case with a larger absolute value of the active-layer thickness requires more time to reach the same degree of coarsening of the coarse layer. This was not visible in the case prior to the flood wave because the situation was close to equilibrium, while this is not the case after the flood wave.

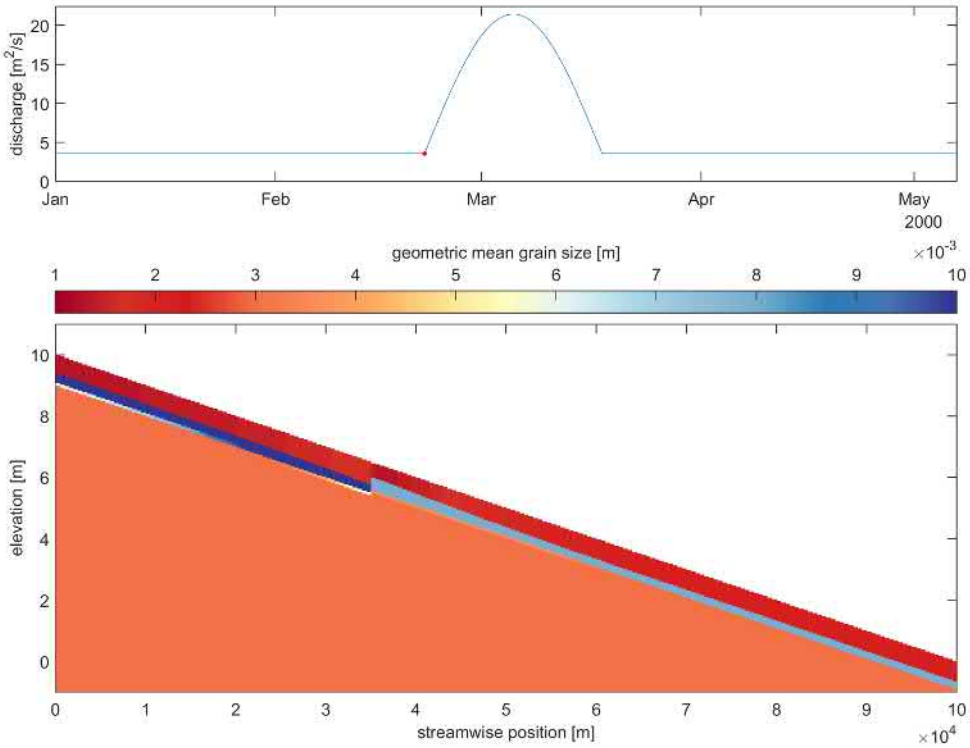

Figure 4.28 Longitudinal profile of the mean grain size before the flood wave in run 05.

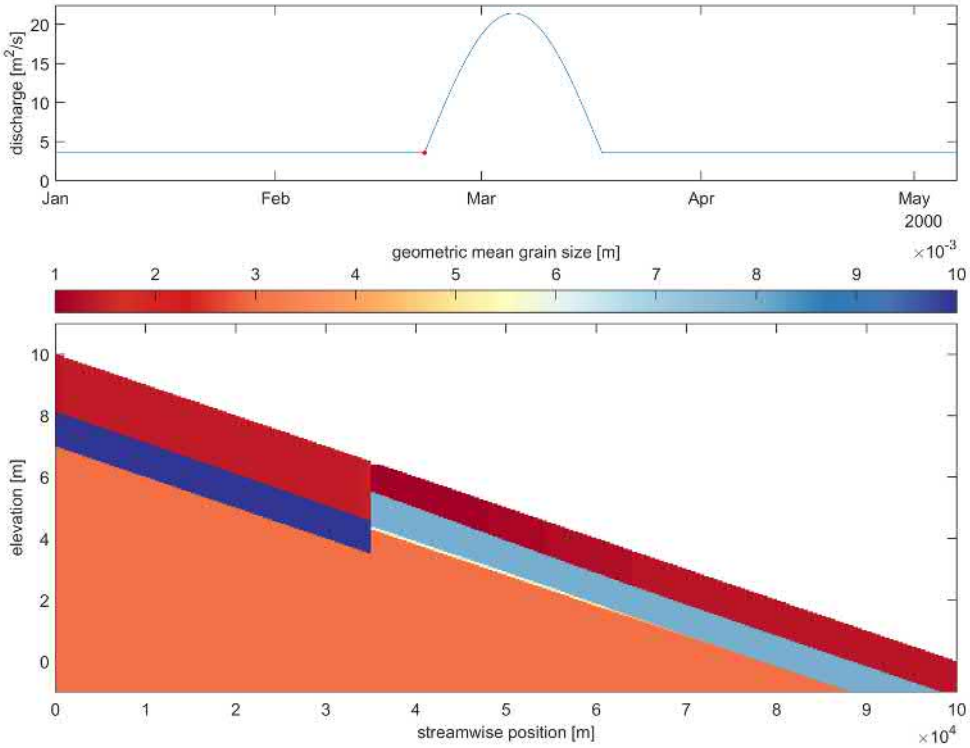

Figure 4.29 Longitudinal profile of the mean grain size before the flood wave in run 09.

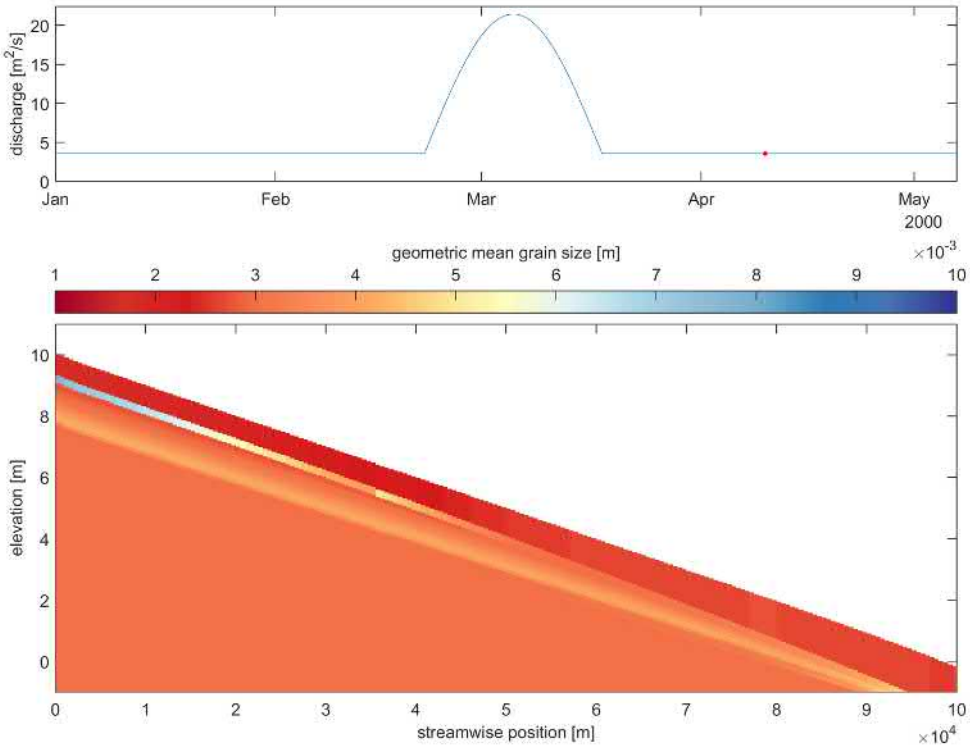

Figure 4.30 Longitudinal profile of the mean grain size at the end of run 05.

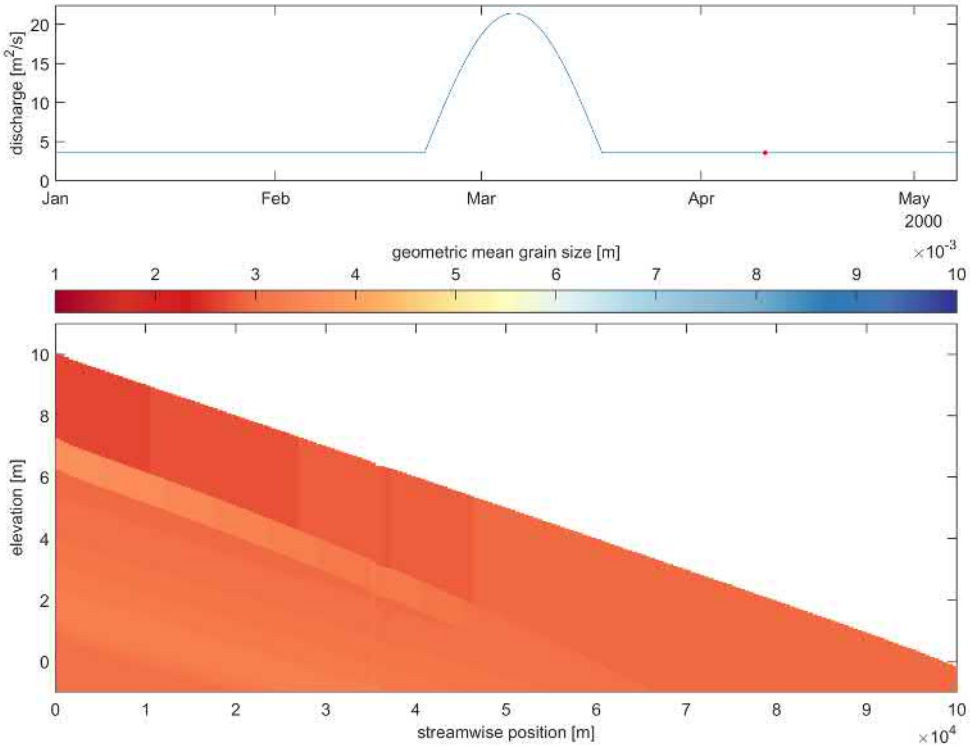

Figure 4.31 Longitudinal profile of the mean grain size at the end of run 09.

4.3.6 Number of size fractions

Simulation 10 models 2 sediment size fractions rather than 5 as in the reference simulation. Although the initial mean grain size is the same, the situation prior to the flood wave is substantially different (Figure 4.32). The coarse sediment size fraction is immobile starting from approximately x =10 km. This fractions amounts to 80% of the total sediment contrary to the reference case, in which immobile sediment after the sudden change (at x =35 km) amounts to 60% of the total. In the case with 2 sediment size fractions the coarse layer forms earlier and the active layer becomes thinner as a consequence. The lack of mobile sediment is so large that there is a point in which the active layer thickness is virtually 0.

At the peak of the flood wave all sediment is mobile and there is barely no stratification. After the flood wave, again the coarse fraction becomes immobile starting from x =10 km deposits in the coarse layer (Figure 4.33). This forms completely in the upstream part contrary to the reference case but does not in the downstream end, as the timescale of immobile sediment deposition increases due to a larger active layer thickness and smaller sediment transport rate. Interestingly, while the reference simulation models coarser fractions than the case with 2 fractions, the coarse layers is much more developed in the latter than the former.

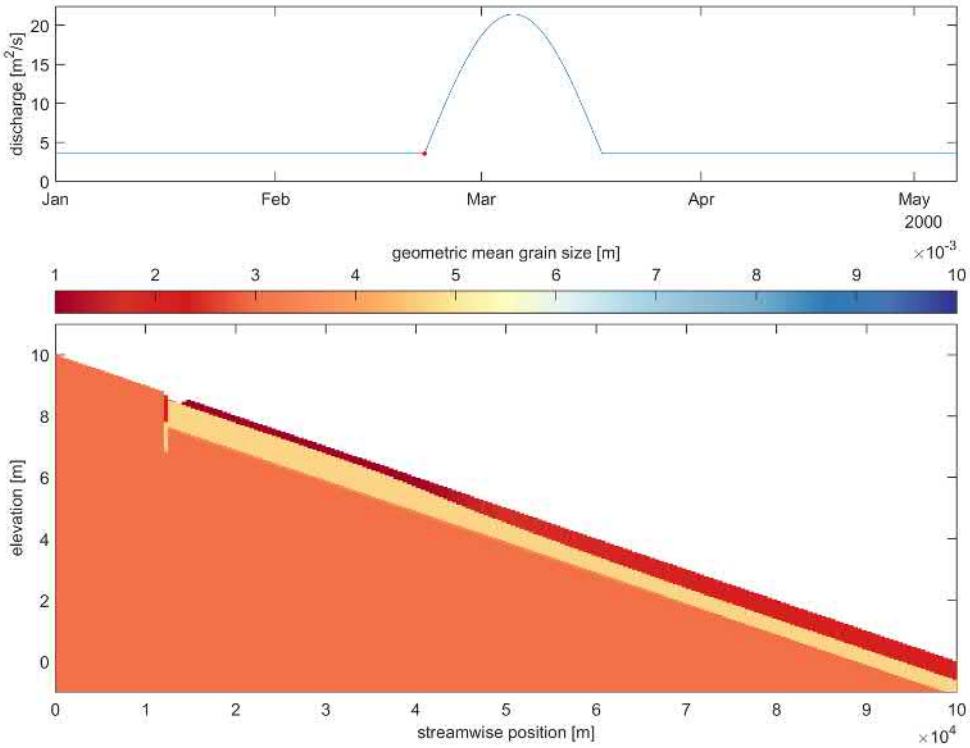

Figure 4.32 Longitudinal profile of the mean grain size before the flood wave in run 10.

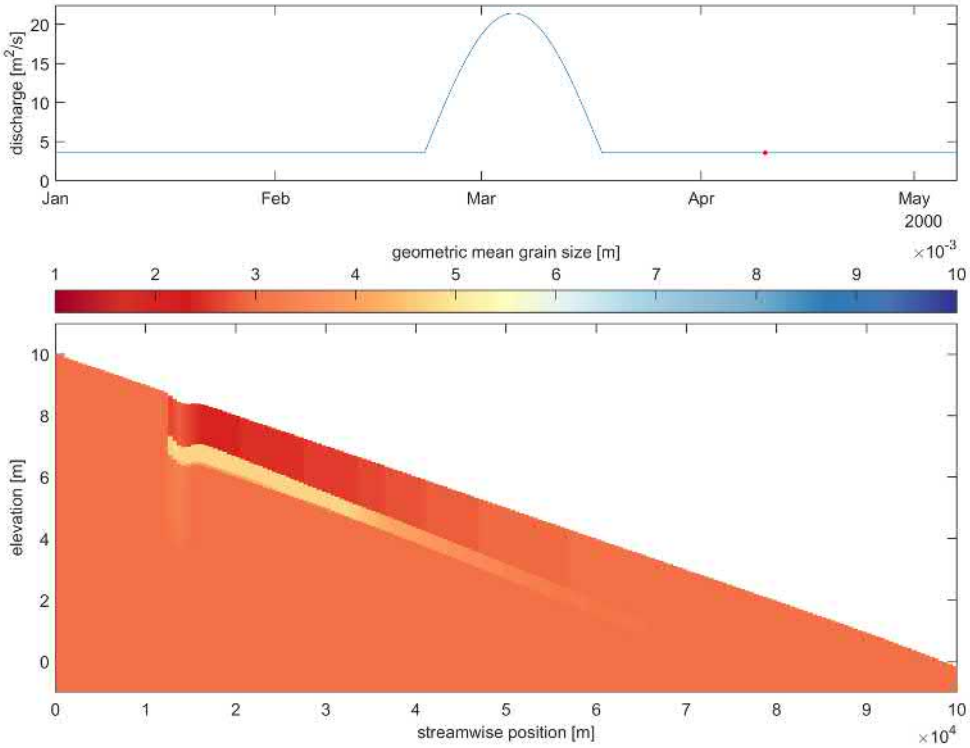

Figure 4.33 Longitudinal profile of the mean grain size at the end of run 10.

4.3.7 Period of the flood wave

The period of the flood wave (Simulation 11) has no effect on the stratification at the peak of the flood wave (Figure 4.34). This is because entrainment of mobile sediment in the coarse layer is instantaneous if the active layer is smaller than the alluvial value relegating the period to an irrelevant variable.

Nevertheless, after the flood wave the stratification is different (Figure 4.35). The coarse layer is less developed and the active layer is coarser. This is due to the fact that the timescale of the flux of sediment between the active layer and the coarse layer is the same in both simulations but the time that passes from the peak until the end of the flood wave is shorter if the period is shorter.

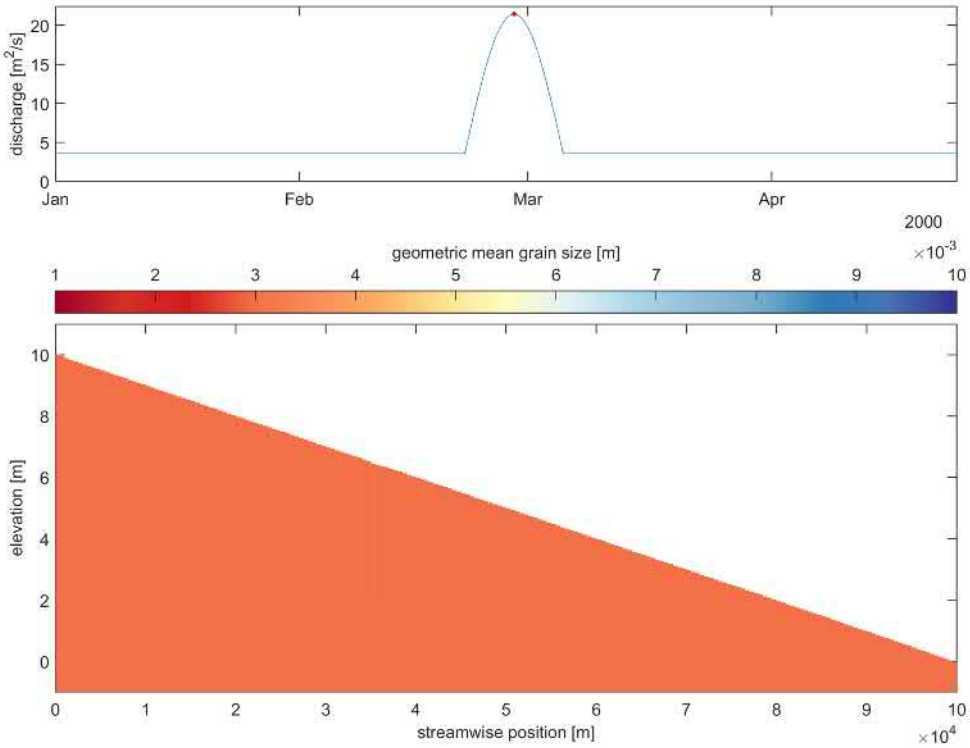

Figure 4.34 Longitudinal profile of the mean grain size at the peak of the flood wave in run 11.

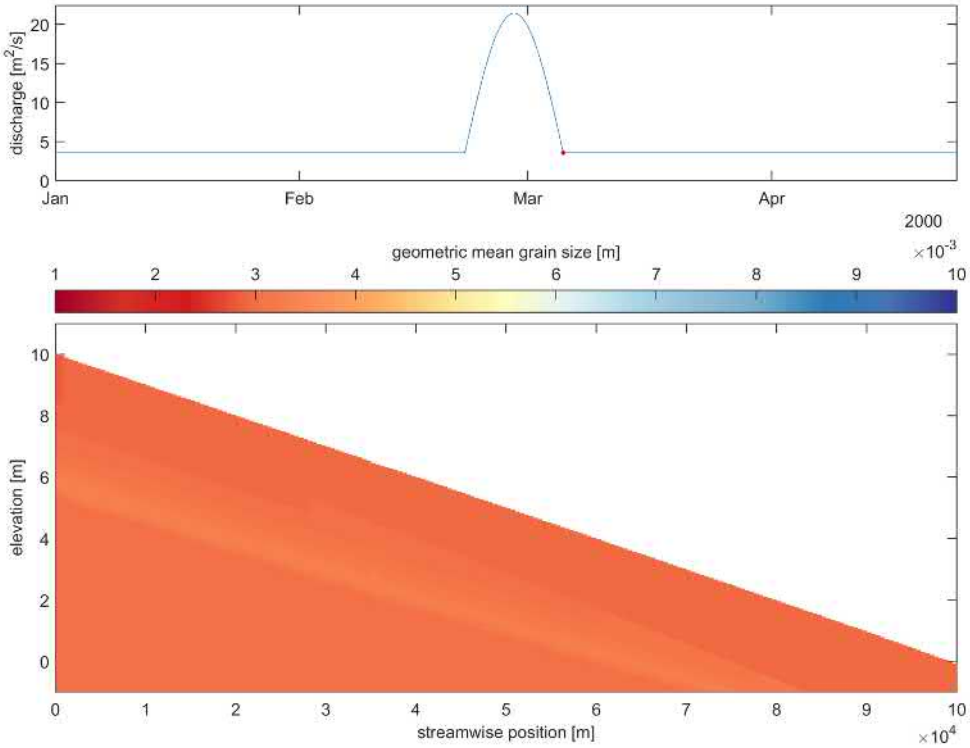

Figure 4.35 Longitudinal profile of the mean grain size after the flood wave in run 11.

4.3.8 Timescale of immobile sediment flux

Simulation 12 is equal to the reference except for the fact that the timescale of the flux of sediment is increases by decreasing the average length between dune troughs. The effect is slightly visible before the flood wave (Figure 4.36). The active layer is slightly finer when the flux is increased. This shows that the reference had not reach equilibrium.

At the peak of the flood wave the situation is the same as entrainment of mobile sediment is instantaneous. After the flood wave there are significant differences. When the flux of sediment is large, coarse sediment is deposited faster in the coarse layer and eventually reaches the substrate as the active-layer thickness decreases (Figure 4.37). Hence, a clearer band of coarse sediment is found in the substrate. This is also clearer at the end of the run (Figure 4.38). It is clearly visible when each sediment size fraction became immobile as it was transferred to the coarse layer and deposited in the substrate forming a band. The coarse layer at the final stage is much more developed than in the reference case.

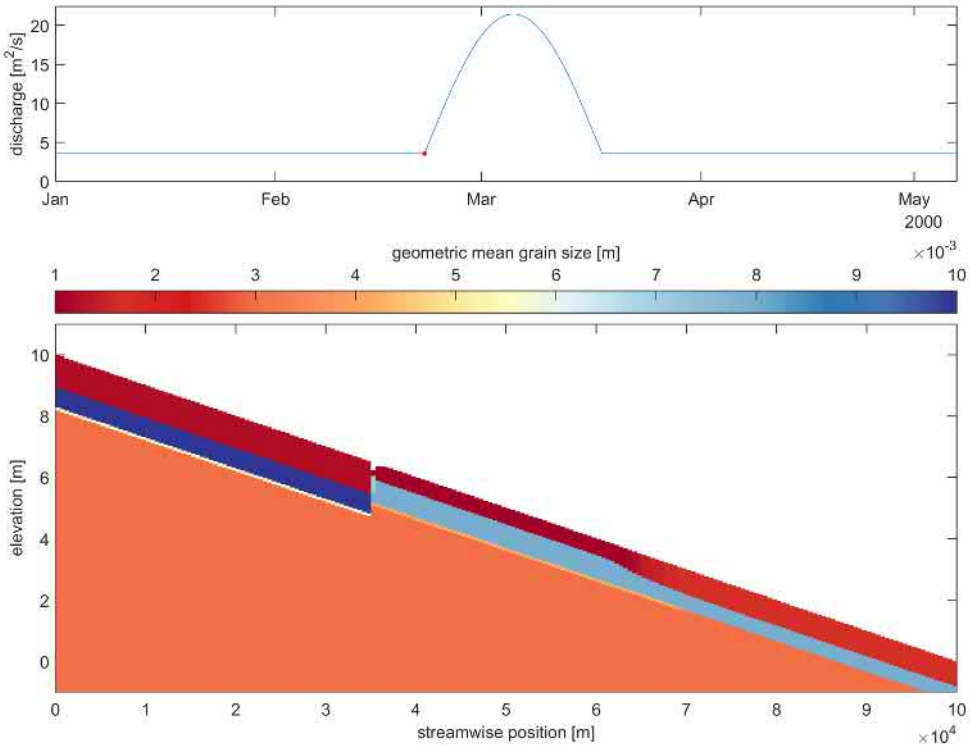

Figure 4.36 Longitudinal profile of the mean grain size before the flood wave in run 12.

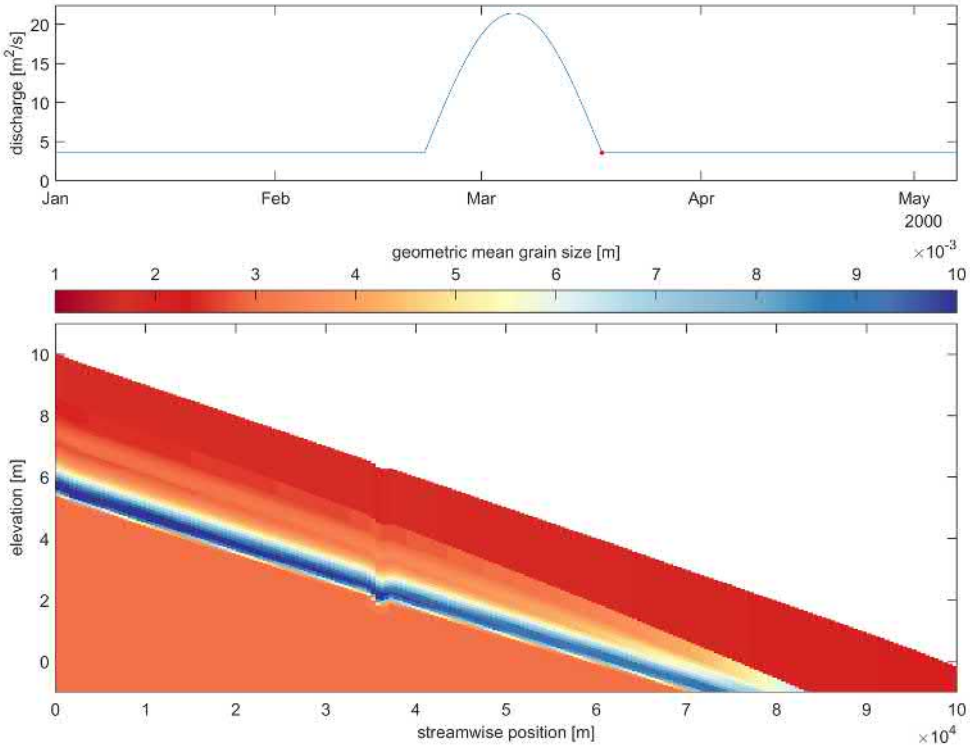

Figure 4.37 Longitudinal profile of the mean grain size after the flood wave in run 12.

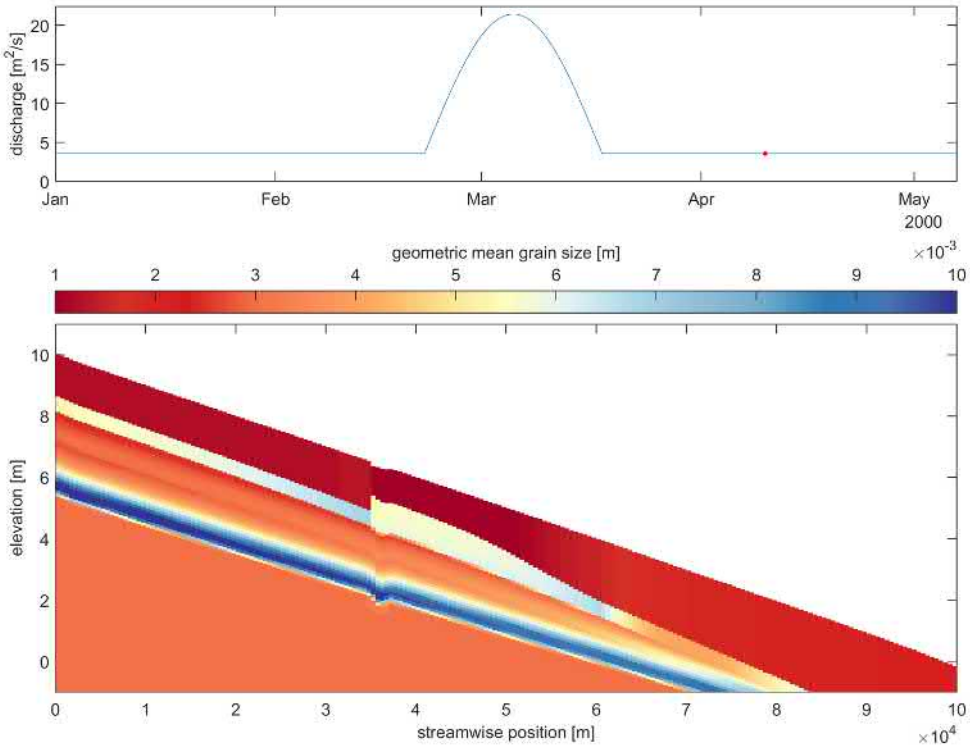

Figure 4.38 Longitudinal profile of the mean grain size at the end of run 12.

4.3.9 Results comparison

Figures 4.39-4.43 present the mean grain size in all cases for comparison.

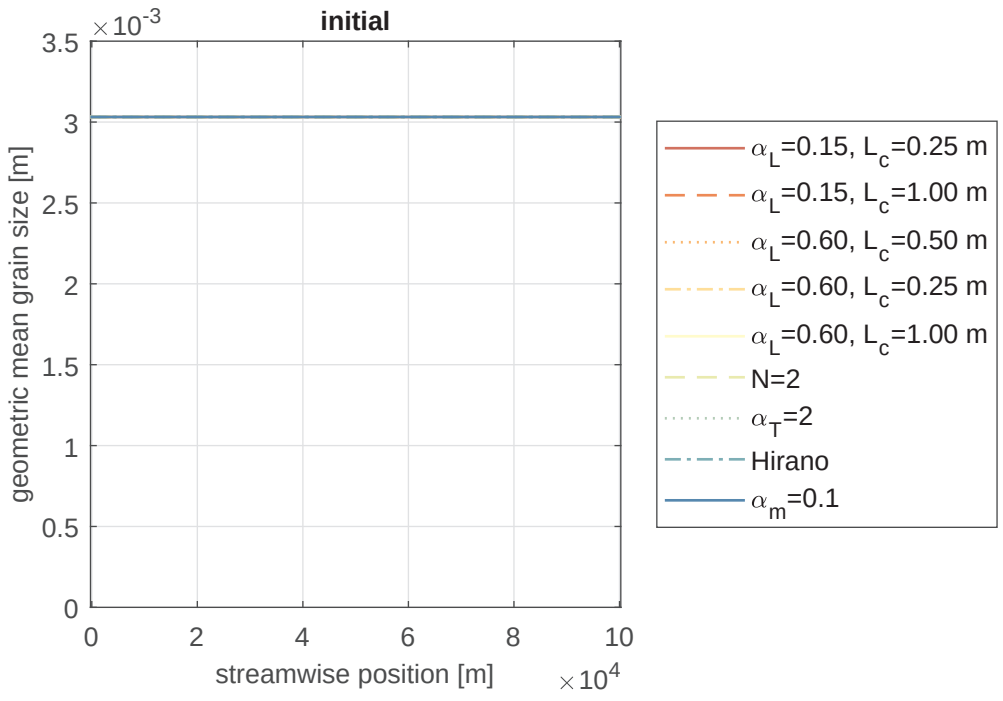

Figure 4.39 Mean grain size of the active layer at the start of the runs.

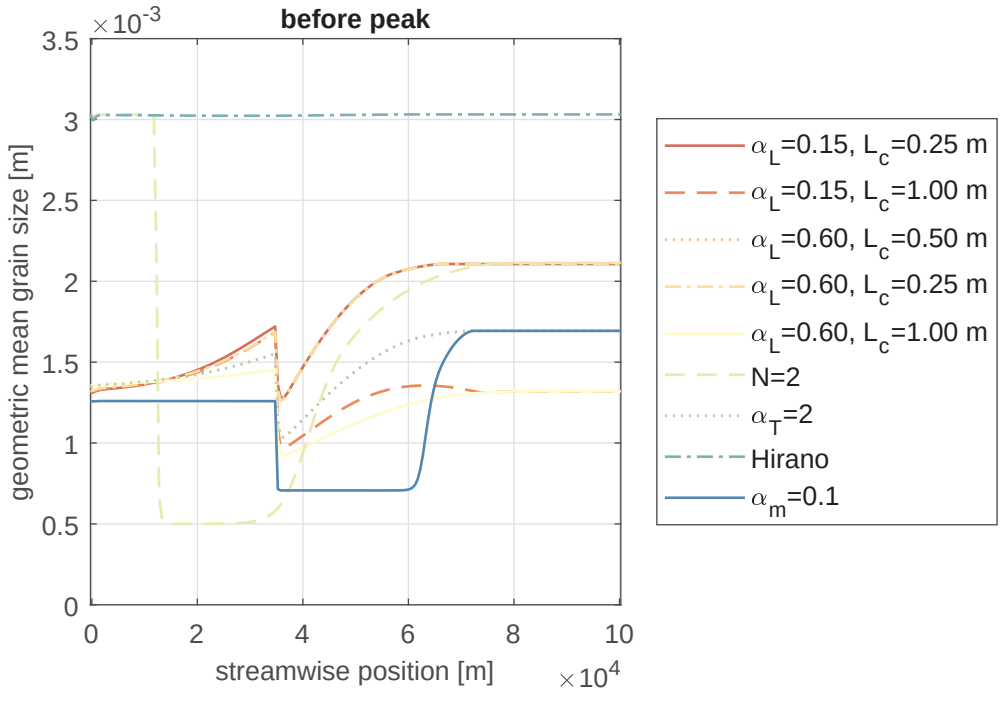

Figure 4.40 Mean grain size of the active layer before the flood wave.

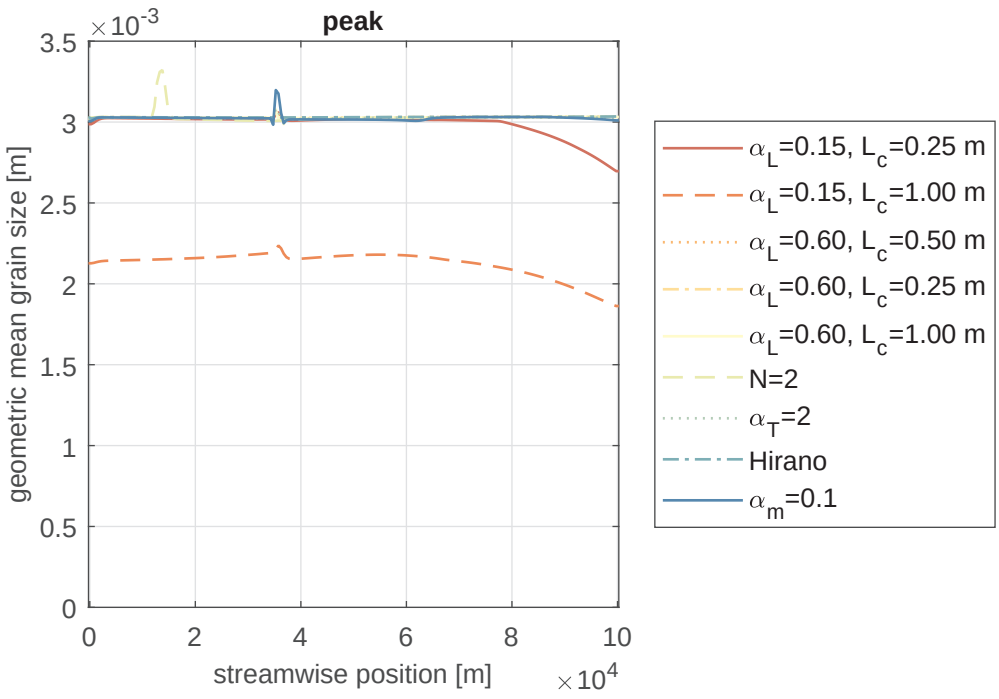

Figure 4.41 Mean grain size of the active layer at the peak of the flood wave.

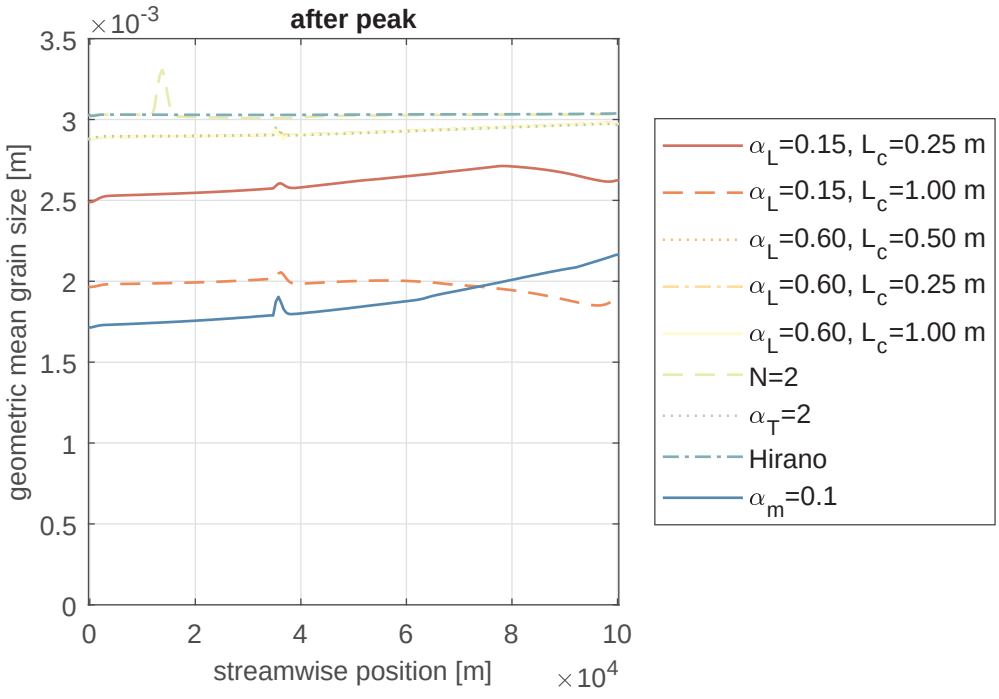

Figure 4.42 Mean grain size of the active layer after the flood wave.

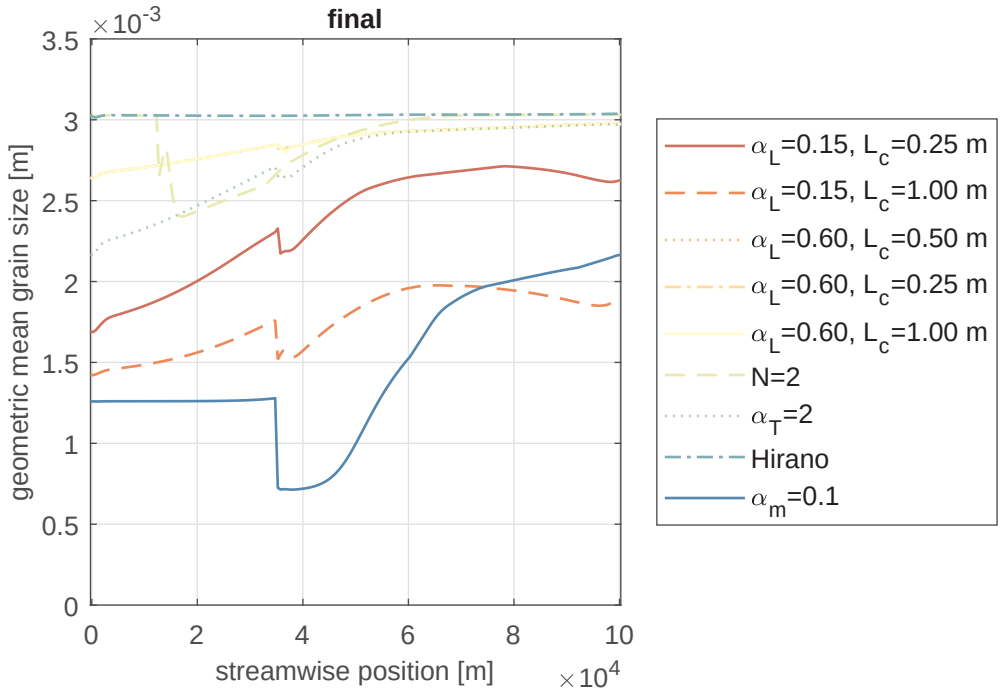

Figure 4.43 Mean grain size at the end of the runs.

5 2D idealized field case

One-dimensional set-ups greatly facilitate the modelling exercises. This is not only because simulations are substantially faster and the analysis becomes simpler, but especially because the complexities due to two-dimensional features such as river bars are eliminated. Nevertheless, these complexities play a role in the usual applications and need to be studied.

For this reason, the two-dimensional consequences of applying the different modelling options are studied in this chapter. To this end, an idealized two-dimensional simulation is set-up in which the bed is unstable to growth of free alternate bars (Colombini *et al.*, 1987; Siviglia *et al.*, 2013). Simulations with constant discharge starting from a flat bed in which part of the sediment mixture is immobile are carried out using both the HANNEKE and the active-layer model.

5.1 Simulation set-up

A straight river with fixed banks is considered. The key parameter controlling growth of free bars is the width-to-depth ratio (Colombini *et al.*, 1987; Siviglia *et al.*, 2013). Hence, in determining the width of the channel, the flow and sediment conditions are first considered. A constant Chézy friction coefficient equal to 37.44 $m^{1/2}/s$ ($C_f = 0.007$) is assumed. Aiming at a depth-averaged velocity equal to 1 m/s and a flow depth of 1 m, the unitary flow discharge is set to 1 m^2/s. This yields an initial bed slope under normal flow conditions equal to 7.1356×10^{-4}. The downstream water level is set to 0 m and the initial bed level at the downstream end to –1 m, such that flow is initially normal. The bed is initially flat in the transverse direction. A random perturbation in bed elevation of order of magnitude equal to 1 cm is applied to accelerate the growth of bars.

Two sediment-size fractions with characteristic grain sizes equal to 0.001 m and 0.01 m are considered. Initially, the bed surface is composed of 50 % of each size fraction. The sediment transport rate is modelled using the relation by Meyer-Peter and Müller (1948) (Equation (3.1)) without hiding-exposure correction. This is because a key ingredient in the simulation is that only fine sediment is mobile and the standard relations (e.g., Egiazaroff (1965)) predict motion of the coarse sediment. The bed-slope effect is modelled using the relation by Koch and Flokstra (1981):

$$g_{sk} = A_s \theta_k^{B_s} \ , \tag{5.1}$$

where A_s $[-]$ and B_s $[-]$ are nondimensional parameters and θ_k $[-]$ is the Shields (1936) stress. Different values of the coefficients A_s and B_s have been proposed (for a review, see Baar *et al.* (2018)). For simplicity we use $A_s = 1$, $B_s = 0$ such that the bed-slope effect is independent from the bed shear stress (Engelund and Skovgaard, 1973; Engelund, 1975).

Using these parameters, the critical width-to-depth ratio is studied analytically by computing the growth rate of the eigenvalues of the linear problem as a function of the wave number (Figure 5.44). The reader is referred to Chavarrías *et al.* (2019) for details on the computation. This figure shows that for a transversal wavelength smaller than 56.6 m there is no growth of perturbations. As the first mode (i.e., alternate bars with wavelength equal to twice the width) is the most unstable, the width must be larger than 28.3 m for bars to grow. A width equal to 30 m is set.

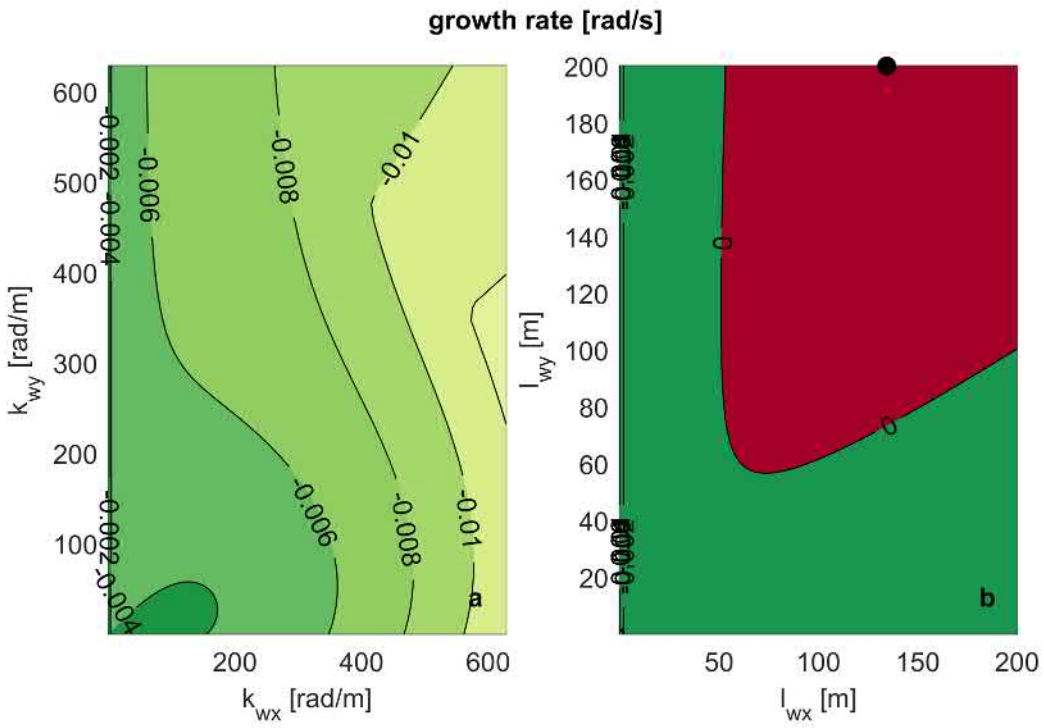

Figure 5.44 Growth rate of perturbations added to the reference case as a function of the wave number and the wavelength. The subplots in the two columns show the same information but highlight the behaviour for large wave numbers (left column) and for large wavelengths (right column). Red and green indicates growth and decay of perturbations, respectively.

The length is equal to 3000 m, which guarantees enough distance for bars to develop. 10 cells are used to discretize the width and 300 for the length. 24 days of morphodynamic development are modelled, which is sufficient for observing alternate bars.

5.2 Simulation plan

The first simulation runs using the active layer model. The active-layer thickness is set to 1 m. The second simulations runs using the HANNEKE model. The alluvial active layer thickness is set to 1 m and the coarse-layer thickness to 0.5 m. Parameter $\alpha_{\mathrm{m}} = 1$, and $\alpha_{\mathrm{L}} = 1$ without loss of generality. As the key parameter identified in the parameter study is the ratio between the alluvial active-layer thickness and the coarse-layer thickness, a third simulation is executed which is equal to the second simulation except for the fact that the coarse-layer thickness is equal to 0.05 m (Table 7).

#	L_a [m]	L_c [m]	model
00	1.0	-	Hirano
01	1.0	0.50	HANNEKE
02	1.0	0.05	HANNEKE

Table 7 Idealized two-dimensional simulations. L_a is the alluvial active-layer thickness in the case of the HANNEKE model.

5.3 Results

Figure 5.47 shows the flow depth in the final state when using the active-layer model. As expected, alternate bars have grown which propagate downstream. The bed surface is approximately composed by 50 % of each size fraction (Figure 5.46). This is reasonable as the only sorting processes are due to streamwise gradients. The composition of fine sediment is in phase with respect to flow depth. At shallow locations (i.e., at the crest of the bars) the composition is finer. The sediment transport rate is composed of only fine sediment (coarse is immobile) and is approximately 1.2 m^2/s (Figure 5.47).

When applying the HANNEKE model with the parameters in Simulation 01, the two-dimensional pattern is approximately the same as when using the active-layer model (Figure 5.48). Bars have grown slightly faster (maximum flow depth around 1.06 m contrary to 1.03 m). Crucially, the composition of the bed surface is completely different, as in this case it is almost entirely composed of fine sediment (Figure 5.49). This is due to the fact that coarse immobile sediment has been deposited in the coarse layer. Still, the transport rate is approximately the same (Figure 5.50).

The fact that the pattern is the same can be explained from the fact that it depends on the sediment transport rate and its derivatives with respect to the flow depth, velocity, and volume fraction content of each size fraction (Chavarrías *et al.*, 2019). The same sediment transport relation is employed in the HANNEKE model and the active-layer model and the coarse layer is thick enough such that the alluvial active-layer thickness is reached. In this case, the sediment transport rate and its derivatives are the same and the linear analysis predicts no difference between the two cases. The differences are due to the transition phase experimented in the HANNEKE model while coarse sediment is being transferred down and replaced by fine sediment.

In Simulation 02 the coarse-layer thickness is significantly reduced, which causes a different pattern (Figure 5.51). In this case, bars are less visible and the amplitude smaller. The thin coarse layer causes the coarse layer to form completely before all immobile sediment has been transferred out of the active layer. As a consequence, the active-layer thickness reduces and the sediment transport rate reduces accordingly, which slows down growth of bars. The sediment transport rate in this case is smaller than in the reference simulation with the HANNEKE model but still comparable to the active-layer model simulation. The difference in pattern between Simulation 00 and Simulation 02 although the transport is similar is explain by the transient period in which large vertical fluxes of sediment occur. Nevertheless, this point requires further study and elaboration.

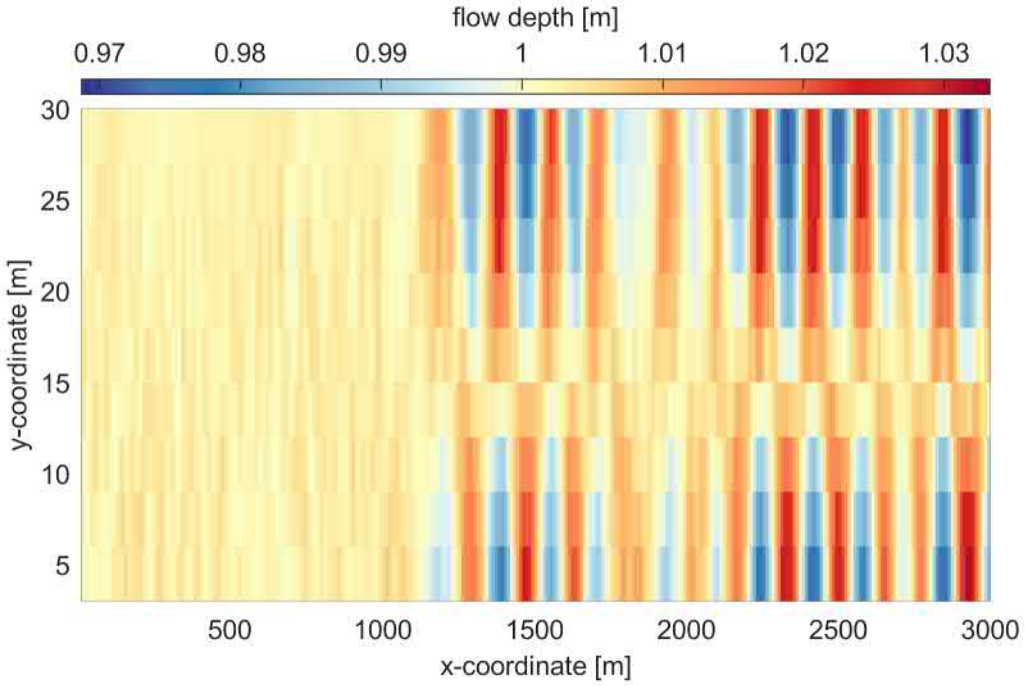

Figure 5.45 Flow depth in the final state in Simulation 00.

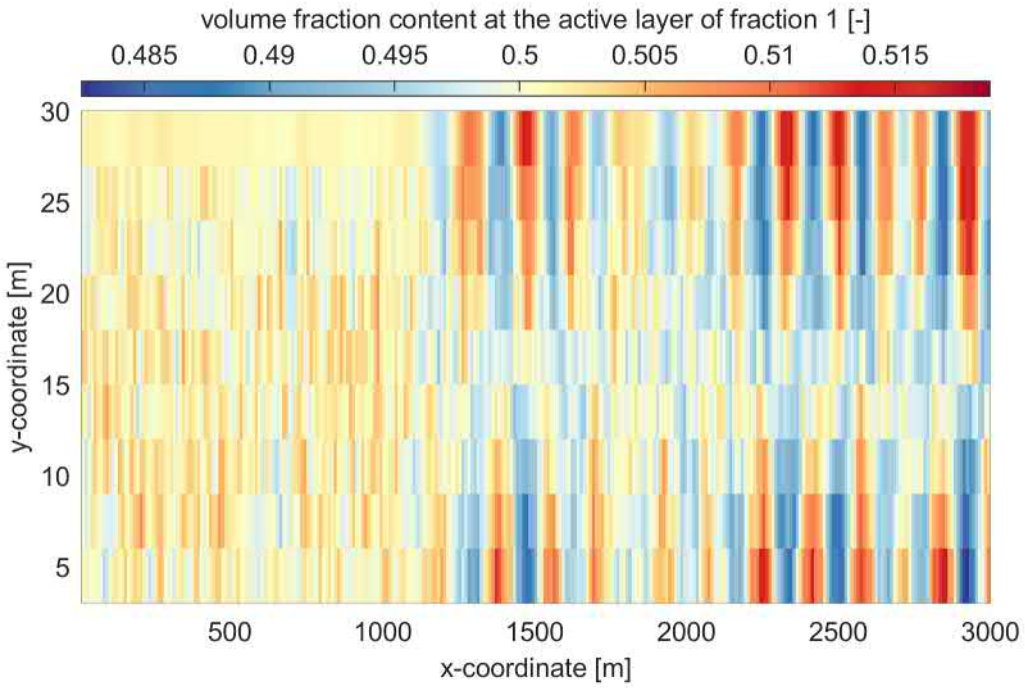

Figure 5.46 Volume fraction content of size fraction 1 in the final state in Simulation 00.

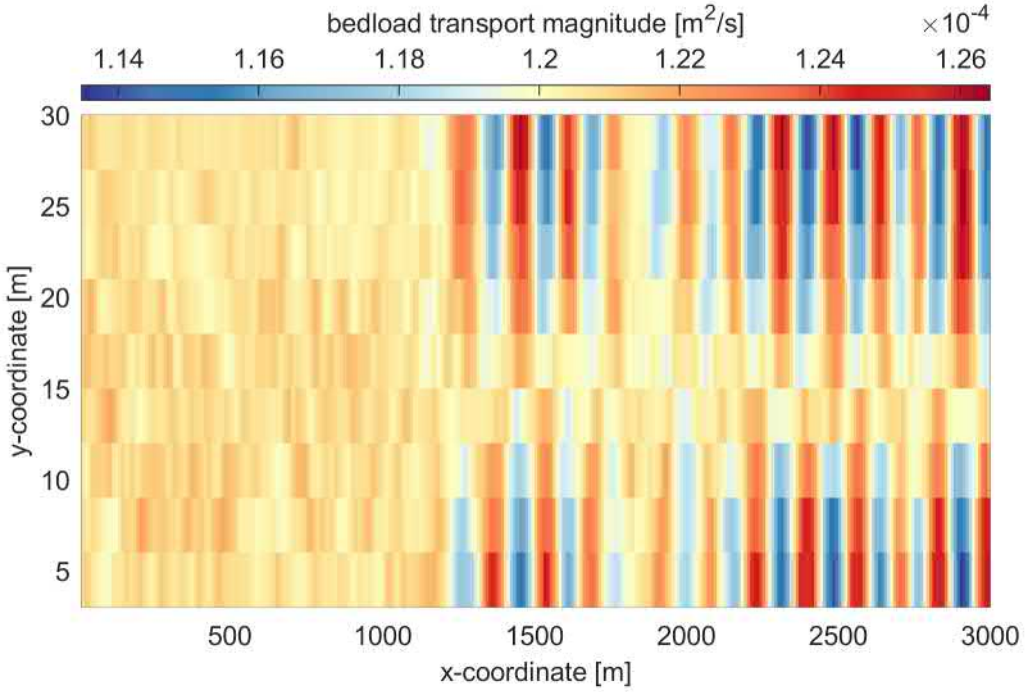

Figure 5.47 Bedload transport magnitude in the final state in Simulation 00.

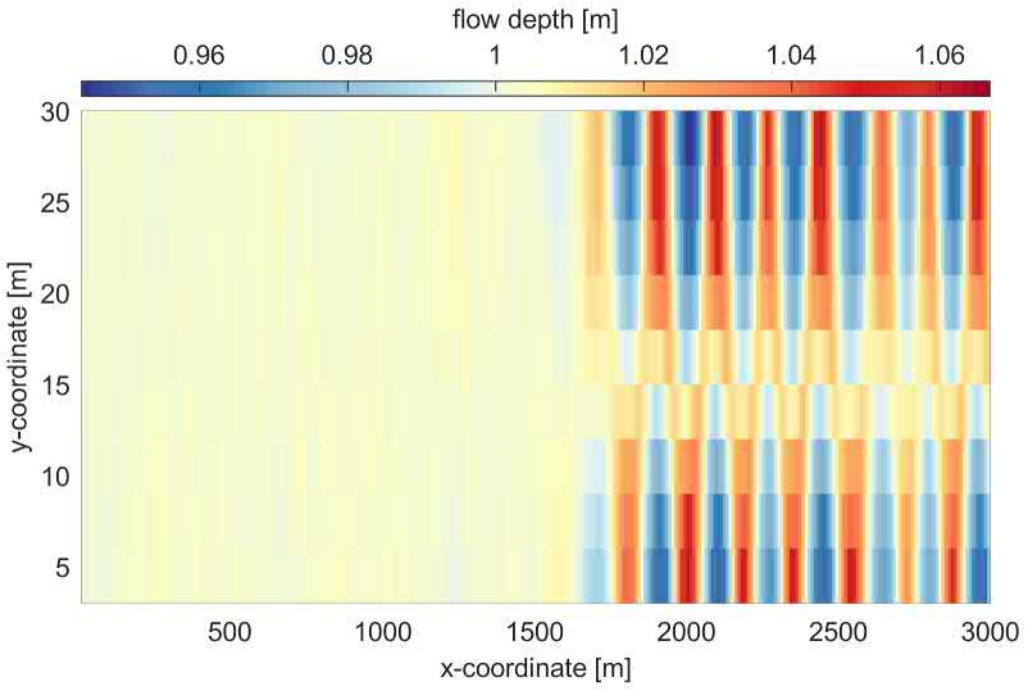

Figure 5.48 Flow depth in the final state in Simulation 01.

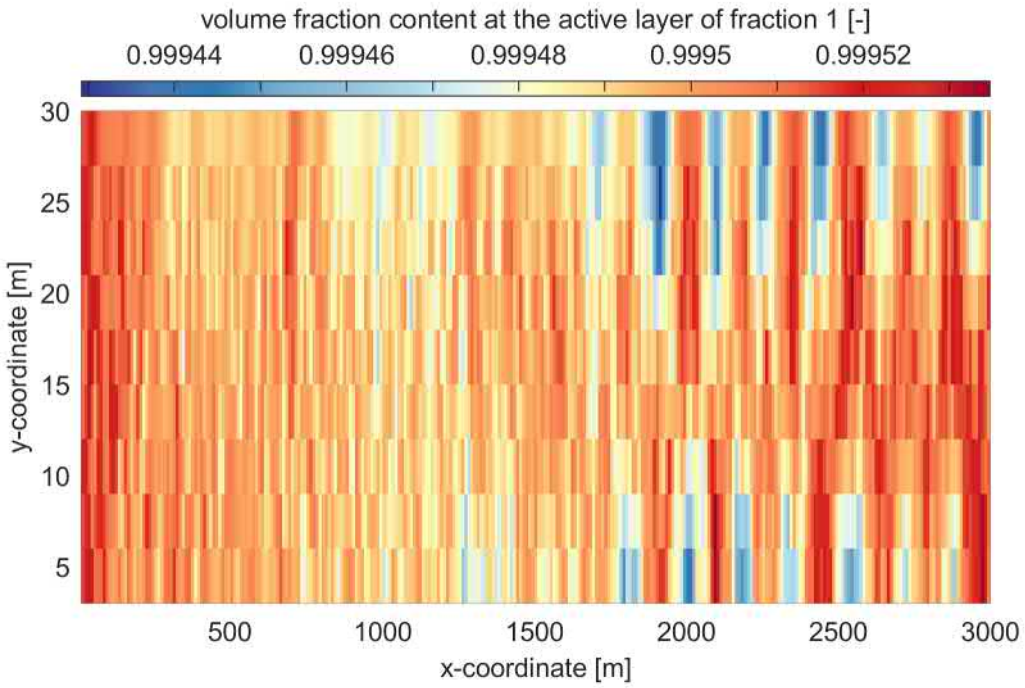

Figure 5.49 Volume fraction content of size fraction 1 in the final state in Simulation 01.

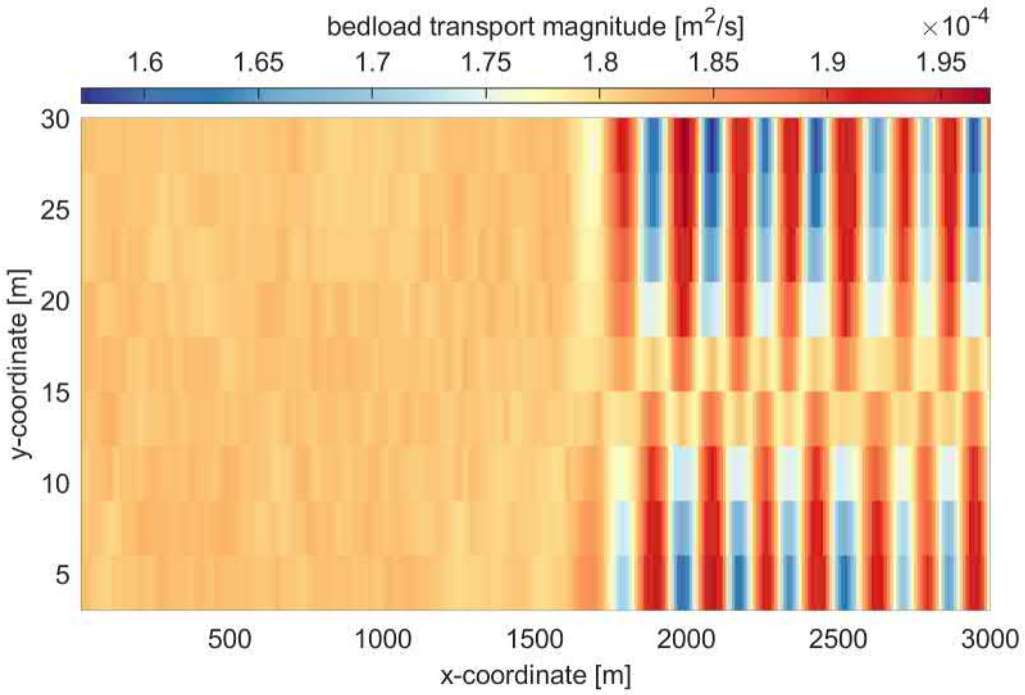

Figure 5.50 Bedload transport magnitude in the final state in Simulation 01.

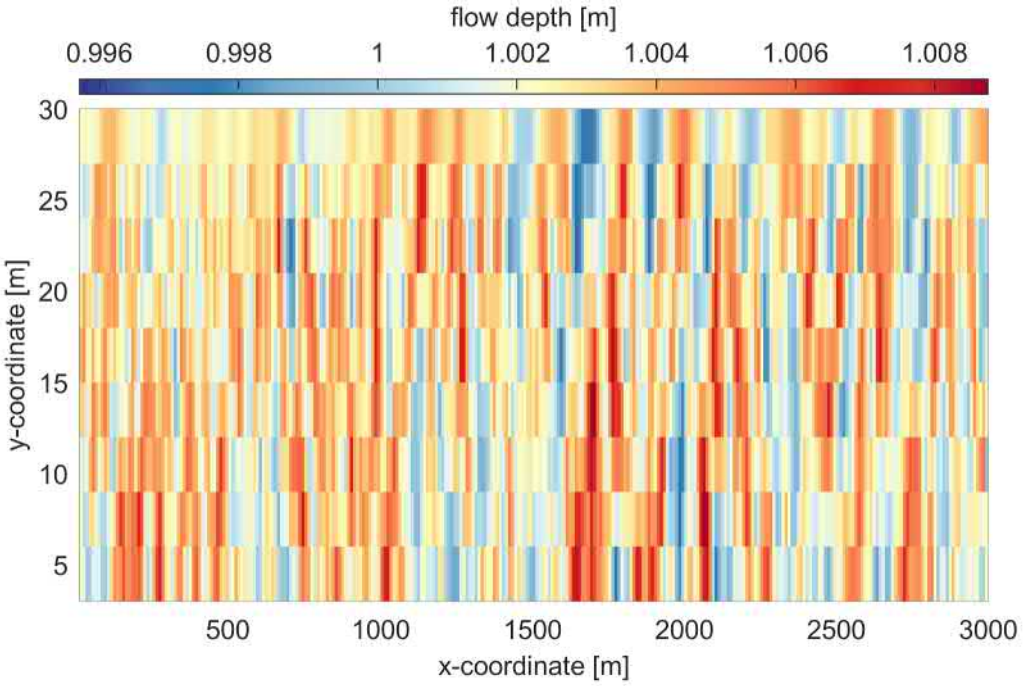

Figure 5.51 Flow depth in the final state in Simulation 02.

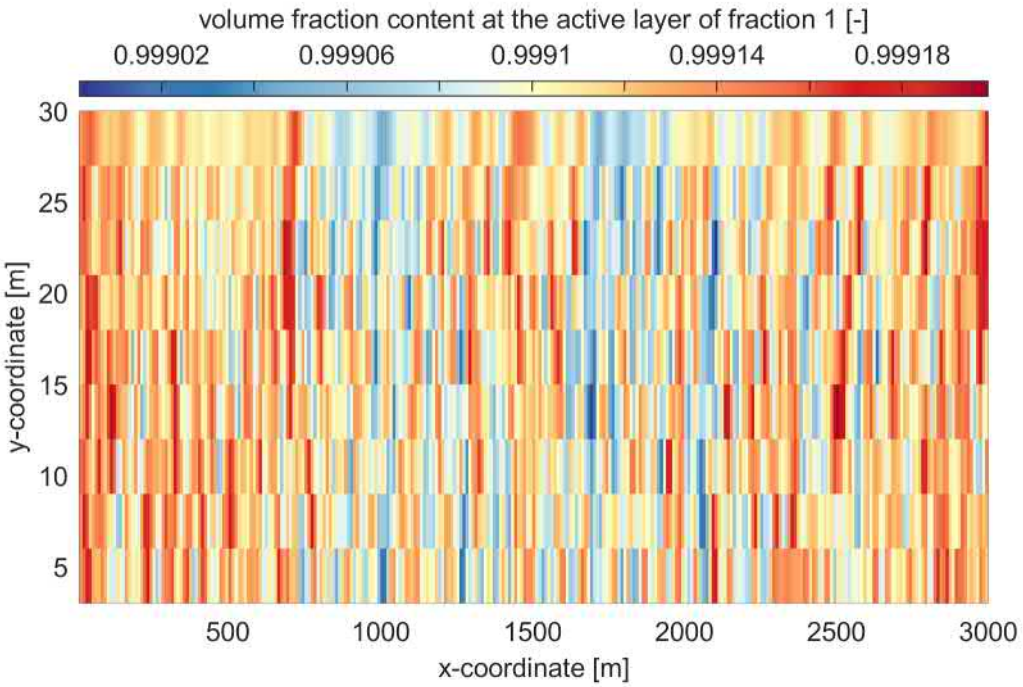

Figure 5.52 Volume fraction content of size fraction 1 in the final state in Simulation 02.

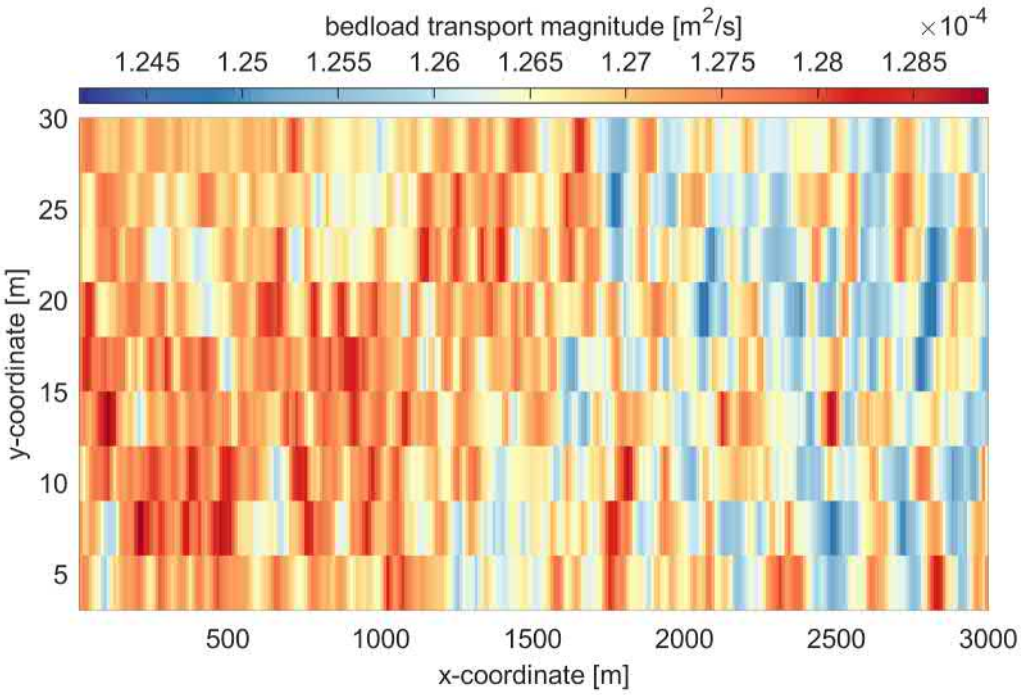

Figure 5.53 Bedload transport magnitude in the final state in Simulation 02.

6 Implications for field modeling

The key results of the study are that:

- The HANNEKE model is crucial for modelling the formation and break-up of a coarse layer.
- The relative thickness between the coarse layer and the alluvial active layer are the main control parameter of the development of a coarse layer.
- A thick coarse layer relative to the alluvial active layer increases the chances that the active layer reaches its alluvial value, as more sediment is available in the coarse layer for exchange.
- A thin coarse layer relative to the alluvial active layer limits the chances that the active layer reaches its alluvial value. As a consequence, the chances of a drastic increase in active-layer thickness due to break-up of the coarse layer increase.
- Given an equal proportion of thicknesses, a larger alluvial active layer thickness in general decreases the stratification, as the timescale of the flux of sediment increases.
- Given an equal proportion of thicknesses, shorter dunes in general increase the stratification, as the timescale of the flux of sediment increases.
- Decreasing the number of size fractions keeping the mean grain size constant may cause different results depending on whether the mean grain size of the lumped fractions is mobile or not at different stages.
- For a case in which the coarsest fractions are lumped together, an expected outcome is that the amount of immobile material increases, causing a coarser coarse layer and limiting the thickness of the active layer.
- The period of a flood wave has not significant effect on the stratification except for the fact that degree of coarsening of the coarse layer depends on the absolute time. Hence, the situation after a flood wave depends on the period of the flood wave.
- The HANNEKE model does not significantly alter the two-dimensional pattern of free alternate bars provided that the coarse layer is thick enough such that the active-layer thickness reaches its alluvial value.
- In the presence of a formed coarse layer which limits the extent of the active-layer thickness to a value below the alluvial one the growth rate of bars is smaller than when employing the active-layer model.

The above results have implications for modelling of field cases. The active-layer model does not explicitly model the formation and break-up of a coarse layer, but does so implicitly with the sediment transport. While the composition of the active layer or substrate does not significantly change during a flood wave, the sediment transport rate does as sediment that is immobile under low flow conditions becomes mobile during the peak of the flood wave. Moreover, the active-layer model is simpler, having less parameters and dependencies than the HANNEKE model. For this reason, the active-layer model should always be used as a benchmark and the results of the HANNEKE model should be interpreted in comparison to the active-layer model.

The HANNEKE model has a large set of parameters that can technically be tuned and calibrated. For the alluvial active-layer thickness, the most reasonable strategy is to relate it to flow depth and tune the prefactor such that the approximate dune height under alluvial conditions as measured in the field is captured.

This is simpler than directly relating it to dune height and computationally faster, as it does not involve solving an advection-diffusion equation. Moreover, what is most relevant is the proportion between alluvial active-layer thickness and coarse-layer thickness rather than the absolute value of the active-layer thickness itself. Certainly, the order of magnitude of the active-layer thickness is crucial, as the celerity of sorting waves depends on it, but the order of magnitude is equally well-captured by a simpler or a complex relation for it.

The number of size fractions seems to be of high importance, but the key is not the number of fractions but the amount of sediment that is immobile. What is key is to properly capture the fraction of sediment that is immobile at every stage. Using a small number of size fractions increases the difficulty of accurately modelling the right proportion of immobile sediment. Moreover, in this case adding one more size fraction may cause large differences in the results. It is suggested to use a large number of size fractions. A test to guarantee that enough size fractions are used could be to split each fraction in two and compare the results. The implications derived from the results should not change when increasing the number of size fractions.

Modelling of hiding-exposure is crucial is capturing the proportion of immobile sediment. This should be calibrated based on measurements. In case it is not possible, the essential point for setting hiding-exposure is that it must capture the change in mobility of the coarsest fractions for the different flow conditions. First the fractions that should be mobile at every stage are to be decided and then hiding-exposure must be set to that end. Once the hiding-exposure is set, it will not have an effect on the number of size fractions given that the mean grain size remains constant. Worded differently, the transport or mobility of a size fraction will not be affected by adding a new size fraction provided that the mean grain size remains constant.

As for the coarse-layer thickness, the thinnest it can be is related is physically related to the size of the coarsest size fractions in the mixture (e.g., the d_{90}). It is reasonable to assume that the part of the bed reworked by the active layer where coarse sediment is deposited is related to the active-layer thickness. The bed is reworked by the troughs of the bedforms and as a consequence it is best interpreted as a fraction of the active-layer thickness. Hence the maximum would be the that it is equal to the alluvial active-layer thickness. Given these limits, the proposed approach is to use it as a calibration. By fixing the alluvial active-layer thickness, the thicknesses proportion is solely controlled by the coarse-layer thickness and it should be set such that the alluvial active-layer thickness is correctly captured under the conditions observed in the field.

Measurements of the sediment transport rate at different stages are scarce but one of the most important metrics for the quality of a morphodynamic model. If available, calibration should not only be based on thickness of the active layer but also on sediment transport for varying discharges. Similarly, the main improvement of the HANNEKE model is the ability to better describe changes in sediment composition. Unfortunately, these measurements are scarce. If available, these should be the main target variable in calibrating the model.

The parameter setting the length of the dunes has a large impact on the timescale of immobile sediment deposition. We would not use this factor as a calibration factor. We consider a better strategy is to calibrate only based on the coarse-layer thickness, assuming a reasonable length of the dunes from measurements (similar to the alluvial active-layer thickness).

If the calibration results are physically unrealistic, (i.e., the coarse layer has an unrealistic thickness) both dune length and height should be revisited.

The study has been limited to a case with a single flood wave. This conveniently limits the simulation time and allows for a broader parameter study. A second flood waves would entrain sediment previously deposited. It would be interesting to study convergence to a dynamic equilibrium with the passing of flood waves depending on the model parameters.

Similarly, the simulation time and the boundary condition imposed upstream (fixed bed) limit the bed elevation changes. It would be interesting to study long simulations with changes in mean bed elevation. This could be done by simply increasing the simulation time as well as with a different boundary conditions upstream causing erosion or sedimentation or introducing a trench in the domain.

7 Conclusions and recommendations

7.1 Summary

The active-layer and HANNEKE models have been applied to a laboratory experiment emulating the stratigraphy created during a flood wave. Only the HANNEKE model is able to capture explicitly the break-up and formation of a coarse layer underneath migrating bedforms. The active-layer model predicts no changes in grain size distribution. Nevertheless, the sediment transport can be used as a proxy for the break-up of an armour layer when using the active-layer model, as immobile sediment suddenly becomes mobile. The application of the HANNEKE model is satisfactory, as it captures the essence of the laboratory experiment.

For gaining understanding on the effect of the model parameters, the HANNEKE model is applied to an idealized one-dimensional case with reference values emulating the Waal River. The alluvial active-layer thickness, coarse-layer thickness, period of the flood wave, number of size fraction and exchange parameter are varied. The ratio between alluvial active-layer thickness and coarse-layer thickness appears to be the key parameter.

The implications of using the HANNEKE model with respect to the two-dimensional pattern are studied using an idealized case. When the active-layer thickness is not limited by the development of a coarse layer, no significant differences arise. The presence of a coarse layer slows down morphodynamic development.

Implications for field scenarios are discussed in combination with the key components to have in mind when using the HANNEKE model.

7.2 Research questions

In this section the research questions are answered.

Under which conditions is the HANNEKE model suitable and necessary? What are the essential differences compared to the state-of-the-art model (i.e, the active-layer or Hirano model)?

Only when interested in modelling mixed-size sediment morphodynamics (i.e., changes in bed composition), the HANNEKE model must be considered. The HANNEKE model provides a more advanced solution compared to the state-of-the-art model (i.e., the active-layer model) only in the presence of immobile sediment. Worded differently, if all sediment is always mobile, there is no added value in applying the HANNEKE model.

The HANNEKE model is strictly necessary when explicitly predicting the formation and break-up of a coarse layer. The alternative active-layer model is incapable of reproducing such a physical process explicitly.

The HANNEKE model is of particular interest when modelling the effect of flood waves. In this case, the HANNEKE model is able to capture the fact that coarse sediment is transferred downwards by flood waves. Such a process is not reproduced by the active-layer model.

In general, the active-layer model does not reproduce vertical sediment fluxes due to, for instance, lee-face sorting mechanisms. Only streamwise gradients in sediment transport per size fraction lead to changes in sediment composition (apart from an increase in active layer thickness when the substrate has a different composition than the active layer). As such, under normal-flow conditions the active-layer model does not predict changes in composition. On the contrary, the HANNEKE model does predict changes in stratigraphy under normal-flow conditions due to deposition of immobile sediment or entrainment of previously immobile sediment.

Which are the most relevant parameters of the HANNEKE model and what is their role? How sensitive are the results to variation in the model parameters?

The sediment transport predictor is key, as it controls whether sediment is mobile or not, as well as the celerity at which sediment is transferred from the active layer to the coarse layer. Nevertheless, the sediment transport predictor is equally important in the standard active-layer model.

The alluvial thickness of the active layer, thickness of the coarse layer, number of size fractions, celerity of flow changes, and timescale of sediment deposition play a relevant point. A description of the effect of each parameters is given in Section 6. From these parameters, the most relevant one appears to be the relative thickness of the alluvial active layer respect to the coarse layer thickness. This controls whether a coarse layer forms or not.

How should the model parameters be chosen?

A limitation of the HANNEKE model is that it has several additional parameters compared to the active-layer model. Moreover, these are not easily measurable not even in a controlled laboratory environment. The proposed approach consist of applying reasonable values based on, in order of preference, field data, laboratory experiments, and expert knowledge, for all parameters except for the coarse-layer thickness, which is then used as a calibration parameter. The calibration should be based on the coarse layer forming and breaking-up at the correct times (or conditions in general). If the calibration procedure leads to physically unrealistic values of the coarse-layer thickness, the suitability of the other parameters should be revised.

7.3 Recommendations

The HANNEKE model has proved to correctly capture the transport of fine sediment over immobile sediment against laboratory data (Chavarrías *et al.*, 2020). In this project it has been shown that it also correctly captures the key physical processes of the formation and break-up of an armour layer against laboratory data. A parameter study has been conducted leading to a clear view of the most important variables as well as a calibration strategy. For this reason, it is recommended to apply the HANNEKE model to a pilot field case as a next step.

From development of the model by (Chavarrías *et al.*, 2020), some points of further development still remain. Currently, the thickness below which the sediment transport rate is reduced (Struiksma's parameter, `THRESH` in Delft3D), is set to a constant parameter. It is necessary that this parameter is linked to the alluvial active-layer thickness. Implementation of this is relatively simple and has been explored, but it should be thoroughly tested.

When the coarse layer moves upwards due to, for instance, an increase in bed elevation under constant active-layer thickness conditions or a decrease in active-layer thickness under constant bed elevation conditions, immobile sediment in the coarse layer moves vertically. This is unrealistic, as immobile sediment should, in essence, be immobile. To overcome this limitation, the flux of sediment from the coarse layer to the substrate under should be composed of immobile sediment only if this exists in the coarse layer.

The active-layer model may be ill-posed (Ribberink, 1987; Chavarrías *et al.*, 2018). When the model becomes ill-posed, the set of equations does not properly represent the physical processes and results should not be trusted. Ill-posed problems develop growing oscillations that scale with the grid. A smaller grid causes faster-growing oscillations that unrealistically mix the bed. Ill-posedness is independent of the numerical solver as it is a limitation of the equations that are solved, and not a problem of how are the equations solved. In other words, it is not a bug and only solving a different set of equations that better capture the dynamics of the situation is a solution.

As the HANNEKE model is a different model than the active-layer model, it could well be that it solves for the problem of ill-posedness. However, this is not the case. When all sediment is mobile there is no difference between HANNEKE and the active-layer model. Hence, at least when all sediment is mobile, the HANNEKE model will also be ill-posed under the same conditions than the active-layer model is. It is possible that the transfer of immobile sediment to a coarse layer underneath the active layer limits the conditions in which the model become ill-posed. This is because, while in the HANNEKE model there is a flux between the substrate and the coarse layer which is the same as between the substrate and the active layer in the active-layer model, the composition of the coarse layer is unaffected by the sediment transport divergence, contrary to the composition of the active layer. Still, this speculation requires a proper study in terms of perturbation analysis.

It is recommended to study the conditions under which the HANNEKE model becomes ill-posed. Furthermore, it is recommended to study whether the regularization strategy for the two-dimensional active-layer model proposed by (Chavarrías, 2019) also regularizes the HANNEKE model.

References

Ashida, K. and M. Michiue, 1971. "An investigation of river bed degradation downstream of a dam." In *Proc. of the 14th IAHR World Congress, 29 August–3 September, Paris, France*, vol. 3, pages 247–255.

Baar, A. W., J. de Smit, W. S. J. Uijttewaal and M. G. Kleinhans, 2018. "Sediment Transport of Fine Sand to Fine Gravel on Transverse Bed Slopes in Rotating Annular Flume Experiments." *Water Resour. Res.* 54 (1): 19–45. DOI: 10.1002/2017WR020604, ISSN 1944-7973, URL http:https://doi.org/10.1002/2017WR020604.

Blom, A. and G. Parker, 2004. "Vertical sorting and the morphodynamics of bed-form dominated rivers: A modeling framework." *J. Geophys. Res., Earth Surface* 109 (F2): F02007. DOI: 10.1029/2003JF000069, ISSN 2156-2202, URL http://dx.doi.org/10.1029/2003JF000069.

Blom, A., J. S. Ribberink and H. J. de Vriend, 2003. "Vertical sorting in bed forms: Flume experiments with a natural and a trimodal sediment mixture." *Water Resour. Res.* 39 (2): 1025. DOI: 10.1029/2001WR001088, ISSN 1944-7973, URL http://dx.doi.org/10.1029/2001WR001088.

Chavarrías, V., L. Arkesteijn and A. Blom, 2019. "A Well-Posed Alternative to the Hirano Active Layer Model for Rivers With Mixed-Size Sediment." *Journal of Geophysical Research: Earth Surface* 124 (11): 2491–2520. DOI: 10.1029/2019JF005081, URL https://agupubs.onlinelibrary.wiley.com/doi/abs/10.1029/2019JF005081.

Chavarrías, V., 2019. *A Regularization Strategy for the Two-Dimensional Active Layer Model*. techreport 11203684-006, Deltares, Delft, the Netherlands.

Chavarrías, V., W. Ottevanger and E. Mosselman, 2020. *Morphodynamic modelling over alluvial and non-alluvial layers. Literature review, update to Tuijnder concept*. Tech. Rep. 11205235-016-ZWS-0006_v0.1, Deltares, Delft, the Netherlands.

Chavarrías, V., W. Ottevanger, K. Sloff and E. Mosselman, 2021. "Modelling morphodynamic development in the presence of immobile sediment." *Geomorphology* .

Chavarrías, V., R. Schielen, W. Ottevanger and A. Blom, 2019. "Ill posedness in modelling two-dimensional morphodynamic problems: Effects of bed slope and secondary flow." *J. Fluid Mech.* 868: 461–500. DOI: 10.1017/jfm.2019.166.

Chavarrías, V., G. Stecca and A. Blom, 2018. "Ill-posedness in modelling mixed-sediment river morphodynamics." *Adv. Water Resour.* 114: 219–235. DOI: 10.1016/j.advwatres.2018.02.011.

Colombini, M., G. Seminara and M. Tubino, 1987. "Finite-amplitude alternate bars." *J. Fluid Mech.* 181: 213–232. DOI: 10.1017/S0022112087002064, ISSN 1469-7645, URL http://journals.cambridge.org/article_S0022112087002064.

Egiazaroff, I. V., 1965. "Calculation of nonuniform sediment concentrations." *J. Hydraulics Div.* 91 (4): 225–247.

Engelund, F., 1975. "Instability of flow in a curved alluvial channel." *J. Fluid Mech.* 72 (1): 145–160. DOI: 10.1017/S002211207500300X.

Engelund, F. and O. Skovgaard, 1973. “On the origin of meandering and braiding in alluvial streams.” *J. Fluid Mech.* 57 (2): 289–302. DOI: 10.1017/S0022112073001163.

Hirano, M., 1971. “River bed degradation with armoring.” *Proc. Jpn. Soc. Civ. Eng.* 195: 55–65. DOI: 10.2208/jscej1969.1971.195_55.

Klaassen, G. J., H. Tukker, J. Driegen and G. van der Woude, 1986. *Morfologie afgepleisterde beddingen: proeven met hoogwatergolven*. Tech. Rep. M2061/Q212, Delft Hydraulics Laboratory, Delft, the Netherlands. (in Dutch).

Koch, F. G. and C. Flokstra, 1981. “Bed level computations for curved alluvial channels.” In *Proc. 19th IAHR World Congress, 2–7 February, New Delhi, India*.

Meyer-Peter, E. and R. Müller, 1948. “Formulas for bed-load transport.” In *Proc. 2nd IAHR World Congress, 6–9 June, Stockholm, Sweden*, pages 39–64.

Parker, G. and P. C. Klingeman, 1982. “On why gravel bed streams are paved.” *Water Resour. Res.* 18 (5): 1409–1423. DOI: 10.1029/WR018i005p01409, ISSN 1944-7973, URL http://dx.doi.org/10.1029/WR018i005p01409.

Parker, G., P. C. Klingeman and D. G. McLean, 1982. “Bedload and size distribution in paved gravel-bed streams.” *J. Hydraulics Div.* 108 (4): 544–571.

Ribberink, J. S., 1987. *Mathematical modelling of one-dimensional morphological changes in rivers with non-uniform sediment*. Ph.D. thesis, Delft University of Technology, Delft, the Netherlands.

van Rijn, L. C., 1984. “Sediment Transport, Part III: Bed forms and Alluvial Roughness.” *J. Hydraul. Eng.* 110 (12): 1733–1754. DOI: 10.1061/(ASCE)0733-9429(1984)110:12(1733).

Shields, A., 1936. *Anwendung der Ähnlichkeitsmechanik und Turbulenzforschung auf die Geschiebebewegung*. Ph.D. thesis, Versuchsanstalt für Wasserbau und Schiffbau, 26, Berlin, Germany. (in German).

Siviglia, A., G. Stecca, D. Vanzo, G. Zolezzi, E. F. Toro and M. Tubino, 2013. “Numerical modelling of two-dimensional morphodynamics with applications to river bars and bifurcations.” *Adv. Water Resour.* 52: 243–260. DOI: 10.1016/j.advwatres.2012.11.010, ISSN 0309-1708, URL http://www.sciencedirect.com/science/article/pii/S0309170812002928.

Struiksma, N., 1999. “Mathematical modelling of bedload transport over non-erodible layers.” In *Proceedings of the 1st IAHR symposium on River, Coastal, and Estuarine Morphoynamics, Genova, Italy*, pages 89–98.